Sedimentary Geology 453 (2023) 106420

Contents lists available at ScienceDirect

Sedimentary Geology

journal homepage: www.elsevier.com/locate/sedgeo

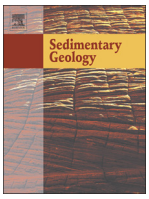

Spatiotemporal variability of the late Paleozoic glacial-to-postglacial transition across eastern Paraná Basin, Brazil

T.E. Mottin [a,*], F.F. Vesely [a], R. Iannuzzi [b], N.P. Griffis [c], I.P. Montañez [c]

[a] Departamento de Geologia, Universidade Federal do Paraná, Curitiba, PR 81531-980, Brazil
[b] Centro de Investigações do Gondwana, Instituto de Geociências, Universidade Federal do Rio Grande do Sul, Porto Alegre, RS 91509-900, Brazil
[c] Department of Earth and Planetary Sciences, University of California, Davis, CA 95616, USA

ARTICLE INFO

Article history:
Received 12 December 2022
Received in revised form 12 April 2023
Accepted 5 May 2023
Available online 13 May 2023

Editor: Dr Massimo Moretti

Keywords:
Glaciation
Climate change
Early Permian
Fossil plants

ABSTRACT

The late Paleozoic glacial-to-postglacial turnover evolved complexly across Gondwana. Successions bearing volcaniclastic material that can be radiometrically dated provide crucial information about the timing of those climate events. The southernmost part of the Paraná Basin, for instance, has a high-precision geochronological framework. The eastern sector of this basin (Paraná State and north of Santa Catarina State), however, lacks radiometric ages, but conversely, has a more complete stratigraphic record, and paleontological information still poorly explored for the purpose of biostratigraphic correlation. This work examines the glacial-to-postglacial interval in the Paraná State, represented by the upper Itararé Group (Taciba Formation; glacial) and lower–middle Rio Bonito Formation (postglacial). Sedimentological, paleontological and geochemical data from outcrops, cores and well logs were used to decipher the timing, paleoclimatic and paleogeographic scenarios of this transition. The examined succession comprises four stacked units (U1 to U4, from older to younger). Diamictite-dominated units (U1 and U3), here interpreted as consecutive glaciation–deglaciation events, are separated by non-glacial, continental to shallow marine deposits, commonly bearing fossil plants and coal seams (U2). An important transgression followed the first deglaciation, which is equivalent to the "*Eurydesma* transgression", based on the presence of marine invertebrates of the homonymous fauna in the Passinho Shale. U2 holds elements of two different floras, i.e., *Phyllotheca–Gangamopteris* (P–G), predating the "*Eurydesma* transgression", and *Glossopteris–Brasilodendron* (G–B), above the transgression. Therefore, U2 is interpreted as an interglacial interval, once it records a climate improving before the last glacial episode of U3, which is further supported by relatively high values of the Chemical Index of Alteration (CIA). Deposits of U3, associated with a decrease in the value of the CIA, are unconformably overlain by U4. The occurrence of coal-bearing postglacial facies (U4) associated with the G–B Flora, coincides with an increase in the CIA values. Sediment transport was toward the SW in all units and in the same direction it is observed an overall thinning of U1 and U3 and thickening of U2. The interglacial P–G Flora of the study area correlates with postglacial southernmost floras, based on U–Pb CA-TIMS Asselian ages of tonsteins. Correlation of the *Eurydesma* fauna-containing Passinho Shale with equivalent successions with high-precision age control in southern Africa, allowed us to position both deglaciations of the Taciba Formation (U1 and U3) in the Asselian. These findings suggest that U1 and U3 record two early Permian glacial episodes, with the younger one (U3) disappearing southward. Accordingly, our results indicate that the glacial-to-postglacial turnover was diachronous along the eastern belt of the Paraná Basin, being progressively older southward, considering that interglacial fossil plant assemblages in the eastern margin correspond in time to postglacial assemblages farther south.

1. Introduction

The late Paleozoic Ice Age (LPIA) and the turnover to a greenhouse state have no parallel in the Earth history, representing the only recorded end of an ice age and the change to a permanent greenhouse condition on a planet characterized by complex terrestrial vegetation (Gastaldo et al., 1996; Montañez and Poulsen, 2013; Limarino et al., 2014). The LPIA is currently envisioned as the longest-lived icehouse (Upper Devonian through much of the Permian), marked by a series of several million-year-long glaciations alternating with interglacial periods with similar duration (Visser, 1997; Isbell et al., 2003, 2012; Montañez and Poulsen, 2013; Montañez, 2022; Fielding et al., 2022).

* Corresponding author.
E-mail address: thammymottin@ufpr.br (T.E. Mottin).

https://doi.org/10.1016/j.sedgeo.2023.106420
0037-0738/

The acme of the LPIA is considered the interval from the late Pennsylvanian to the early Permian (López-Gamundí et al., 2021; Montañez, 2022). The stratigraphic record of this phase is widespread throughout Gondwana, with evidence that the glaciers and ice-sheets may have reached sea-level (e.g., Visser, 1997; Isbell et al., 2008; Rocha-Campos et al., 2008; Montañez and Poulsen, 2013; Montañez, 2022; Fielding et al., 2022). Transition to fully postglacial conditions has been considered to be influenced by the interplay of multiple factors, including the northward drift of Gondwana during the late Paleozoic (Powell and Li, 1994), rise of pCO_2 (e.g., Montañez et al., 2007; Richey et al., 2020) and topography (e.g., Isbell et al., 2012; Goddéris et al., 2017).

Vegetation underwent significant changes during this period, apparently in step with climate shifts (Cúneo, 1996; Gastaldo et al., 1996). Close to the Carboniferous–Permian boundary, for instance, the Gondwanan vegetation, hitherto very impoverished and dominated by typical late Carboniferous forms, was succeeded by a glossopterid-dominated flora, with an increased number of plant assemblages and taxa (Cúneo, 1996). In this context, Brazilian Paleozoic sediments bear one of the most important records of Gondwanan terrestrial floras (Iannuzzi, 2010, 2013).

In the Paraná Basin of central–southern Brazil, a complete record of the late Paleozoic glacial demise and the onset of the postglacial state is preserved in strata of the Itararé Group and the Rio Bonito Formation (Mottin, 2022). High-precision U–Pb ages recently obtained in the southernmost Paraná Basin (Rio Grande do Sul and central Santa Catarina; Cagliari et al., 2016; Griffis et al., 2018, 2019a, 2021) have motivated the idea that glaciation is limited to the Carboniferous and that the turnover to a postglacial state was probably a synchronous event throughout the basin (Griffis et al., 2019a, 2019b, 2021), thus diverging from the model that depicts glaciation and deglaciation as dynamic, diachronous and influenced by local factors (e.g., Isbell et al., 2012).

The Paraná is a huge, continental scale basin that covered different paleolatitudinal zones during the LPIA. Moreover, tectonic modifications close to the Carboniferous–Permian boundary caused profound changes in sediment dispersal patterns (e.g., Milani, 1997; Mottin et al., 2018; Mottin, 2022). Unfortunately, the lack of high-precision ages in most part of the basin makes the proposition of the synchronous glacial–postglacial shift difficult to be confirmed or rejected. Therefore, stratigraphic correlation through the integration of physical, chemical and biostratigraphy supported by a paleogeographic setting can help to test this hypothesis in the absence of confident geochronological control.

This work is part of the Ph.D. project conducted by the first author and composes one chapter of the respective thesis (Mottin, 2022). It aims to present a regional stratigraphic framework of the late Paleozoic glacial-to-postglacial transition tied to paleontological, paleocurrent and paleoclimatic data, from an eastern perspective of the Paraná Basin. The study area corresponds to the Permo-Carboniferous outcrop belt in the Paraná State (Fig. 1). Correlations between key fossil-bearing stratigraphic sections (this work) with recent high-precision geochronological datasets of fossil-bearing sections of southern Brazil and southern Africa (Griffis et al., 2018, 2019a, 2021; Cagliari et al., 2023) allowed constraining the timing of important sedimentary-climatic events in the eastern margin of the basin.

2. Geological background

The Permo-Carboniferous sedimentary succession of the Paraná Basin has long been considered an interesting research topic, extensively examined during almost 150 years (e.g., Derby, 1878). The main reasons are economic, related to coal deposits and potential source rocks and hydrocarbon reservoirs, and scientific, on account of its accumulation during a major climate shift of glacial to postglacial conditions in the Paleozoic Era.

The deposition related to the shift from glacial to postglacial conditions in the Paraná Basin occurred at mid-paleolatitudes of Gondwana (~50–52°S, Franco et al., 2012; Brandt et al., 2019), in a time range spanning the Middle–Upper Pennsylvanian to the Artinskian (Cagliari et al., 2014, 2016, 2023; Griffis et al., 2018, 2019a). This interval includes an important part of the longest-lived and most acute icehouse of the Earth history, the late Paleozoic Ice Age or LPIA (Fielding et al., 2008; Limarino et al., 2014; Montañez and Poulsen, 2013; Montañez, 2022), and the complete transition to a postglacial stage, represented in the Paraná Basin, respectively by the Itararé Group and Rio Bonito Formation.

The Itararé Group comprises up to 1300 m of continental, transitional and marine deposits with variable degrees of glacial influence, that are archives of multiple ice expansions and retreats across southwestern Gondwana (e.g., Rocha-Campos, 1967; França and Potter, 1988; Santos et al., 1996). Deglaciation cycles consisting mostly of diamictites, sandstones, and dropstone-bearing mudstones were described across the basin (e.g., França and Potter, 1988; Vesely and Assine, 2006; Valdez Buso et al., 2019). According to França and Potter (1988), the Itararé Group records three major depositional cycles of basin scale, corresponding to the Lagoa Azul, Campo Mourão and Taciba formations, in ascending stratigraphic order. This stratigraphic scheme is adopted in this work. Most of the deposition of the Itararé Group is considered Pennsylvanian, but some authors extend the unit up to the early Permian based on biostratigraphy of marine invertebrates and palynology (Taboada et al., 2016; Souza et al., 2021). However, data on U–Pb geochronology suggest that the final deglaciation in the southern to southeastern Paraná Basin (locality 4 in Fig. 1A) is prior to the Carboniferous–Permian boundary (Cagliari et al., 2016, 2023; Griffis et al., 2018).

Deposition of the coal-bearing Rio Bonito Formation followed the final deglaciation of the Itararé Group. Across the eastern outcrop belt, the contact between those units is a subaerial unconformity (Zacharias and Assine, 2005) that passes southwards to a correlative conformity where mudstones from the uppermost Itararé Group are genetically linked to heteroliths and sandstones from the lowermost Rio Bonito Formation (e.g., Medeiros and Thomaz Filho, 1973; Castro, 1991; Schemiko et al., 2019). The Rio Bonito Formation is subdivided, from base to top, into the Triunfo, Paraguaçu and Siderópolis members (Schneider et al., 1974). The Triunfo Member comprises fine- to coarse-grained sandstones and subordinate conglomerates, mudstones, coaly shales and coal. The intermediate member, Paraguaçu, encompasses mainly mudstones, with interspersed fine-grained sandstones and limestones. The Siderópolis Member is composed of very fine- to fine-grained sandstones, shales, and coal seams (Schneider et al., 1974). The unit increases in thickness southwards, while the Itararé Group becomes thicker toward the north (Holz et al., 2010).

3. Methods

Outcrops and well cores representative of the interval between the Taciba Formation and lower Rio Bonito Formation, located between northeast Paraná State and northern Santa Catarina State (Fig. 1B) provided the bulk of the dataset used in this work. In addition to these primary data, we used a stratigraphic log from Ibaiti (Zacharias and Assine, 2005) and paleobotanic data from Teixeira Soares (Oliveira, 1927; Read, 1941; Almeida, 1945; Dolianiti, 1948, 1954).

In order to characterize the stratigraphic stacking pattern and its vertical and lateral variability along the area, four composite stratigraphic profiles at 1:100 scale (Teixeira Soares, Ibaiti, Tomazina, Ribeirão Novo) were constructed, three well cores were described at 1:100 scale (PP-11-SC, FP-08-PR, NF-09-PR) and gamma-ray logs were used to help defining textural trends (PP-13-PR, IV-10-PR, PP-17-PR, RS-02-01/80, 1-CA-03-PR, CP-08-02, 1-SJ-1-PR and AS-20-PR wells).

The studied succession was subdivided into informal lithostratigraphic units, hereinafter referred to as units (U1–U4), defined and characterized on the basis of their lithologic properties or combination of

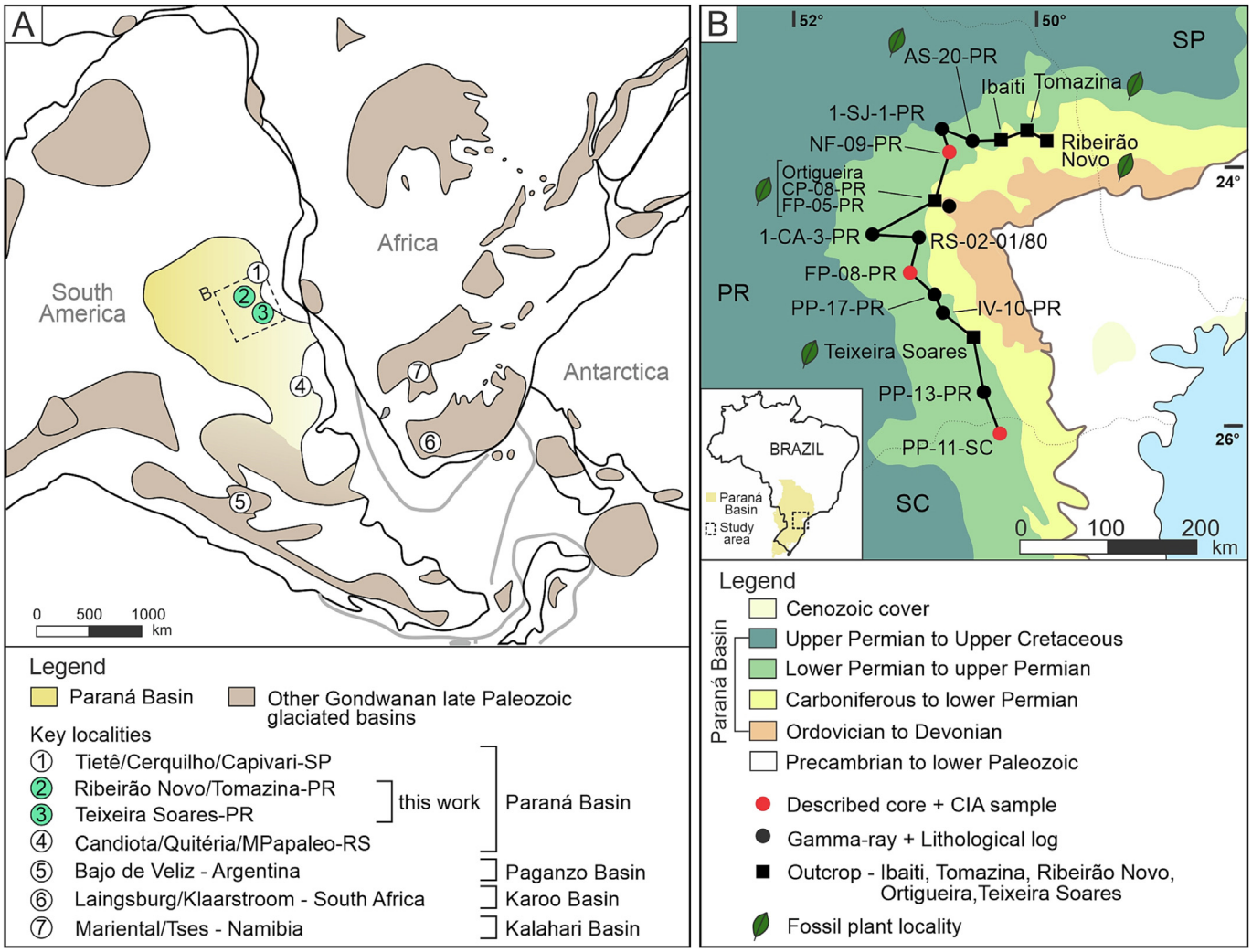

Fig. 1. Geological setting. (A) Overview of the southwestern Gondwana (modified from Isbell et al., 2003) showing glaciated basins during the LPIA, among which the Paraná Basin, and seven key localities addressed in this paper. The approximate location of the study area and two studied key localities is represented by a dashed line polygon and green circles (2–3), respectively. (B) Magnified view of the study area in the eastern part of the Paraná Basin, showing the location of outcrops, fossiliferous localities, described cores, CIA samples and well logs used herein.

lithologic properties, and their stratigraphic relations (Salvador, 2013). The units are mappable and traceable throughout the study area, each one characterized by one or more facies associations. Their boundaries were placed at positions of major lithologic changes (Salvador, 2013). The units were defined by examining the stratigraphic columns from outcrops, cores and nearby exposures distributed in the four main outcrop locations (Fig. 1). UTM coordinates of studied outcrops and cores are presented in Supplementary data 1. A regional correlation of lithostratigraphic units was established using the base of U3 as datum, once it represents a significant increase in water depth as seen in the Discussion section, can be readily identified in outcrops, cores and well logs, and is traceable throughout the study area.

Paleocurrent data were measured in cross stratification and ripple cross lamination in sandstones of different facies associations, totaling 953 measurements (Supplementary data 2). Among the paleobotanical materials examined by the authors, the samples from Ribeirão Novo are housed at the Museu de Paleontologia of the Departamento de Paleontologia e Estratigrafia, Instituto de Geociências, Universidade Federal do Rio Grande do Sul (UFRGS), having originally been described by Guerra-Sommer et al. (1981) and re-examined in this work. The other samples recently recovered by some of authors (TM, FFV, RI) from Teixeira Soares and Tomazina have not yet been cataloged.

The Chemical Index of Alteration (CIA; Nesbitt and Young, 1982), a proxy for the degree of chemical weathering of soils and sediments, was calculated for 30 subsurface samples of mudstones collected from cores of PP-11-SC, FP-08-PR and NF-09-PR wells (Fig. 1B).

Chemical weathering on continents is controlled by moisture and temperature levels. Regions under arid and polar climates demonstrate weak chemical weathering because of limited precipitation and cold temperatures (Wang et al., 2020), and the detritus produced in this setting is similar in composition to the source rocks. In contrast, in tropical and temperate settings, chemical weathering is substantially higher, leading to the removal of mobile cations and concentration of Al in the weathered materials.

The CIA as proposed by Nesbitt and Young (1982) is defined by the following equation:

$$CIA = 100 \times (Al\_2\ O\_3)/(Al\_2\ O\_3 + CaO* + K\_2\ O + Na\_2\ O)$$

where all the elemental concentrations are expressed in moles, and the CaO* refers only to CaO in the silicate minerals (Fedo et al., 1995), thus excluding the CaO in carbonates and phosphates.

The correction, following that in Wang et al. (2020), considers that: 1) CaO is corrected for that residing in apatite using P_2O_5 data ($CaO' = CaO - 10 / 3 \times P_2O_5$); 2) if CaO′ is greater than Na_2O, the final CaO* value is considered equal to Na_2O; and 3) if CaO′ is less than Na_2O, the final CaO* is considered equal to CaO′. The concentration of major elements was measured using a PANalytical PW1480 Wave Dispersive

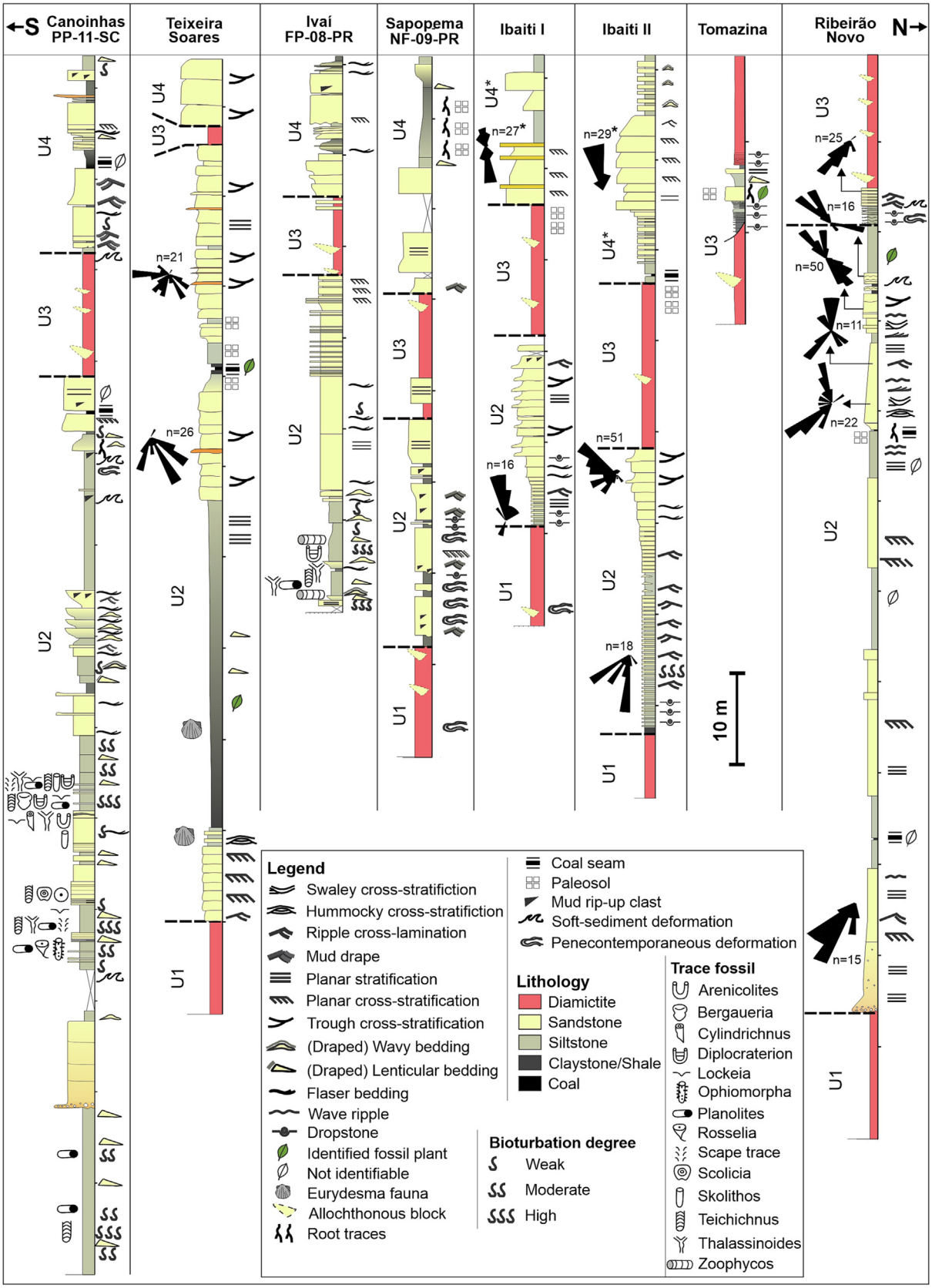

Fig. 2. Stratigraphic sections described from outcrops (Teixeira Soares, Ibaiti, Tomazina and Ribeirão Novo) and well cores (Canoinhas, Ivaí and Sapopema), showing the boundaries between units and their sedimentary facies. Paleocurrents are represented by black vectors next to the corresponding facies. The number of measurements is indicated. *Stratigraphy and paleocurrents modified from Zacharias (2004).

X-Ray Spectrometer at the SGS Geosol Laboratory in Minas Gerais, Brazil. Loss-on-ignition (LOI) was measured at 1000 °C for all samples. Raw and processed geochemical data for the 30 samples are given in Supplementary data 3.

4. Results

4.1. Stratigraphic framework

The study interval is about 140 m thick, includes the upper Taciba Formation and the lower Rio Bonito Formation, and comprises four stacked units (U1 to U4) (Figs. 2–7). A unit as referred to herein encompasses multiple facies associations, each characterized by distinct sedimentary facies and formed in different depositional environments (Mottin, 2022). Description, interpretation, thickness and fossil content of facies associations encompassed by each unit are presented in Table 1.

The units can be traced for at least 450 km, between the Ribeirão Novo locality and the Canoinhas well core (PP-11-SC; Fig. 3). The bounding relationships between units are mostly sharp, characterized by abrupt vertical facies changes (Figs. 2–3). Lateral changes of facies are present mainly within U2 and U4, whereas U1 and U3 are laterally homogeneous, consisting basically of diamictites (Figs. 2–3).

4.1.1. Unit 1 (U1)

U1 comprises the basal deposits of the studied succession. Its thickness varies from 10 m (Teixeira Soares) to 15 m (Ribeirão Novo; Table 1; Fig. 2) and consists of diamictites characterized by polymictic clasts (granules to boulders up to 1.2 m) immersed in a muddy to muddy–sandy matrix (Fig. 4). Clasts are predominantly of crystalline rocks, especially granite, quartzite, rhyolite, and gneiss, among which faceted, striated and bullet-shaped clasts are common (Fig. 4A, E, G, H–J). Three facies were recognized, including massive diamictites, banded diamictites with rare dropstones, and diamictites with allochthonous blocks.

Massive diamictites (Fig. 4A–B, J) are characterized by a homogeneous silty to sandy–muddy matrix. Diamictites with a banded matrix consist of remnants of sandy (white) and muddy (gray) beds with diffuse contacts (Fig. 4C). Occasionally it can show lonestones deforming the underlying strata, i.e., dropstones (Fig. 4E). Soft-sediment deformations are abundant in banded diamictites, including different types of folds, faults, and sand injectites (Fig. 4C). Metric to decametric intrabasinal blocks of conglomerates and sandstones with variable degrees of deformation characterize the third facies of this unit (Fig. 4D, F, K).

4.1.1.1. Interpretation. Massive diamictites with faceted/striated clasts may have multiple origins, including direct emplacement by a glacier, ice rafting and resedimentation of glacial material via debris flows (e.g., Visser, 1989, 1994; Gama Jr. et al., 1992; Eyles et al., 1993). However, the association of massive diamictites, diamictites with deformational structures and allochthonous blocks in U1, suggests the origin of this unit as gravity flows, specifically slumps (e.g., Mottin et al., 2018; Valdez Buso et al., 2019; Rodrigues et al., 2020, 2021). U1 can thus be interpreted as a mass-transport complex composed of resedimented glaciomarine material. The presence of glacially abraded clasts, exotic boulders and dropstones points to the relative proximity of an ice margin at the time of deposition.

4.1.2. Unit 2 (U2)

U2 is laterally traceable for at least 450 km and attains a maximum thickness of 103 m in the Canoinhas well core (PP-11-SC). This unit has sharp lower and upper contacts and is between two diamictite-dominated units, corresponding to U1, below, and U3, above (Figs. 2–3).

U2 is highly heterogeneous (Table 1; Fig. 5) and more typically characterized by a coarsening-upward pattern (Fig. 2). The main facies are cross-stratified, laminated and massive sandstones, bioturbated and

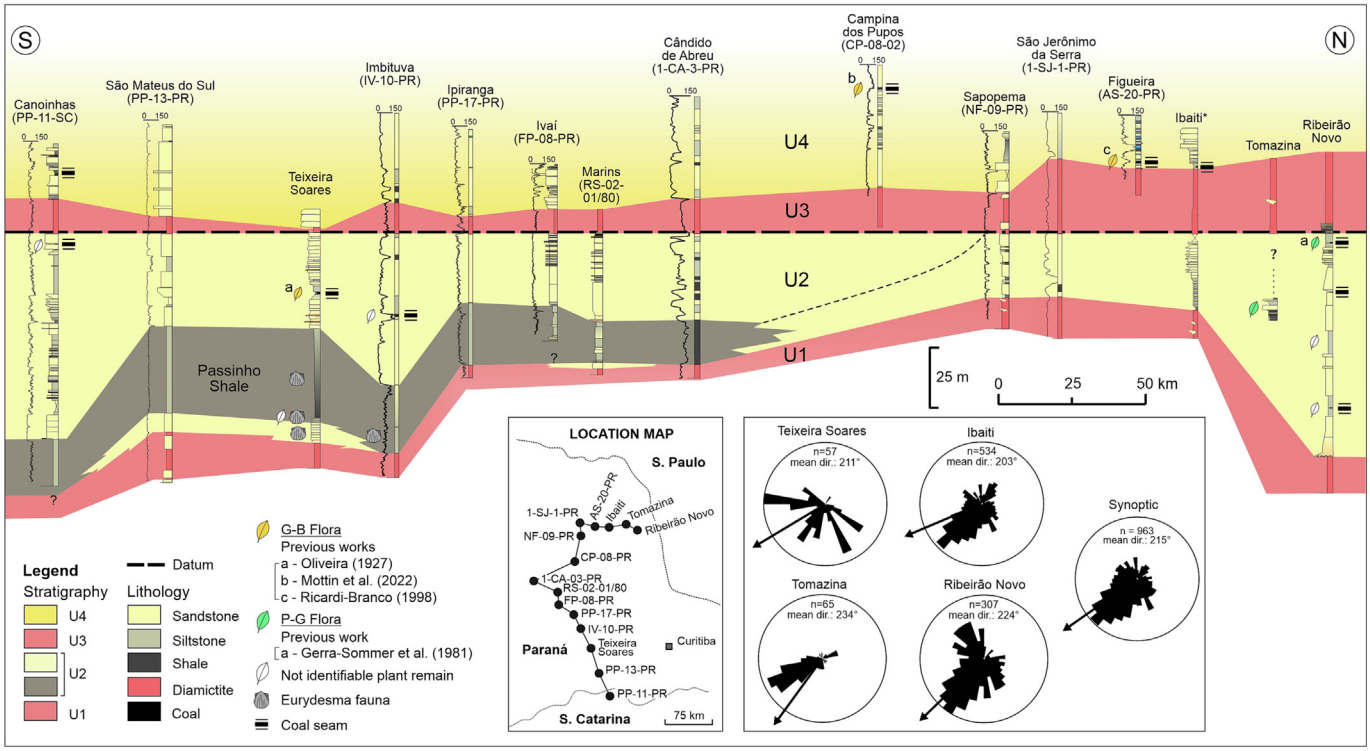

Fig. 3. S–N correlation panel of the study interval, i.e., U1 to U4, using outcrop sections, well cores and well logs. Fossiliferous levels and coal seams are represented next to the stratigraphic interval of occurrence. G–B Flora = *Glossopteris–Brasilodendron* Flora; P–G Flora = *Phyllotheca–Gangamopteris* Flora (floras according to Iannuzzi and Souza, 2005). Paleocurrents are from cross-stratified and current rippled facies and reflect fluvial and deltaic sediment dispersal.

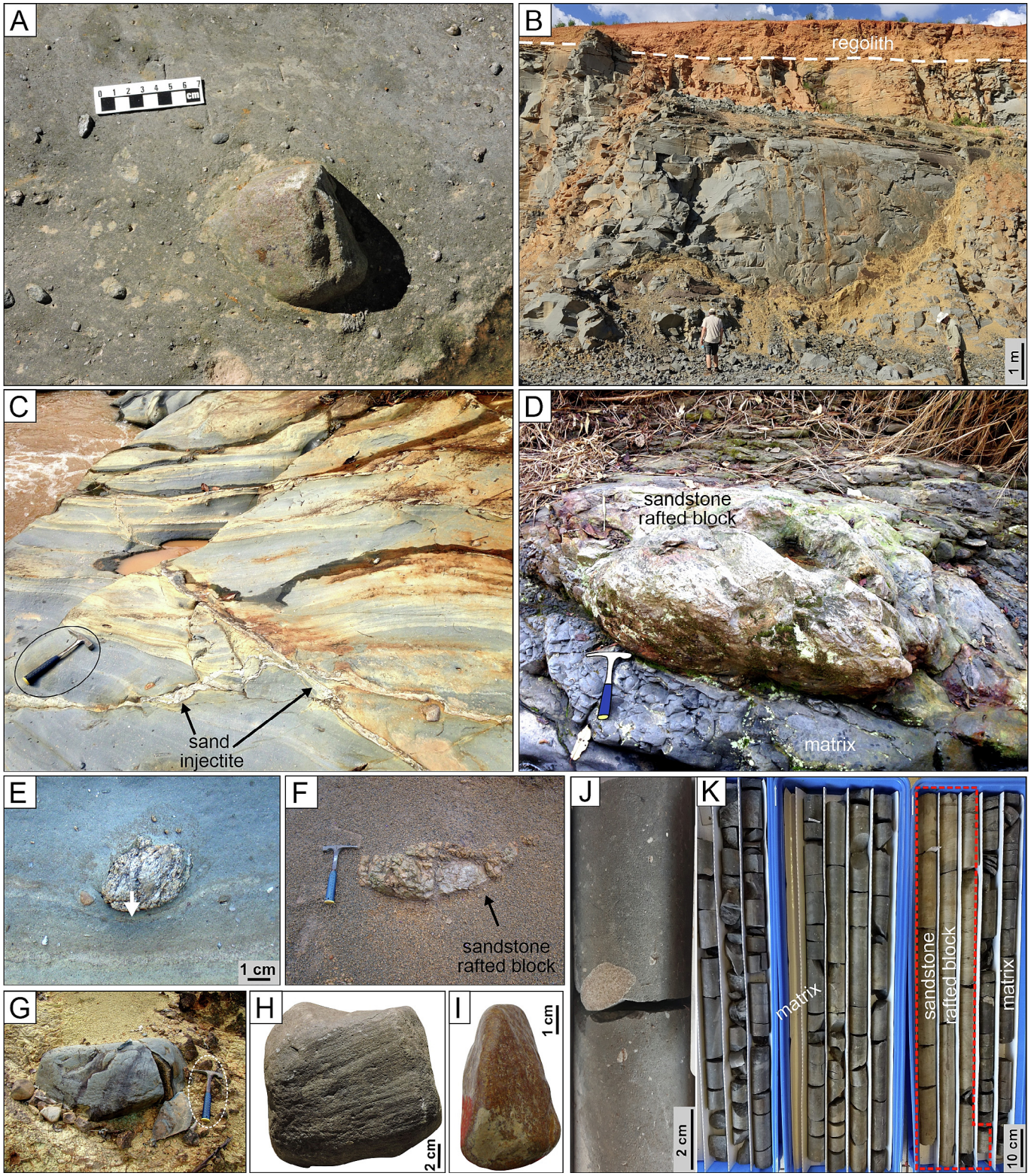

Fig. 4. U1. (A) Granule- to cobble-sized angular clasts in massive diamictite described in Ibaiti. (B) Massive diamictite quarry of U1 in Teixeira Soares. (C) Banded and resedimented diamictite cut by sand injectites (D) Resedimented diamictite showing a metric sandstone rafted block in a sandy–muddy matrix. (E) Granite dropstone deforming sandy layer in banded and resedimented diamictite, Ibaiti. (F) Lenticular sandstone raft in a muddy matrix of resedimented diamictite. (G) 90 cm long clast of crystalline rock observed in resedimented diamictite in Ibaiti. (H) Striated and (I) bullet-shaped clasts retrieved from diamictites of U1. (J) Massive diamictite facies with granitic granules to pebbles, Sapopema well core. (K) 3 m-thick sandstone rafted block (red dashed polygon) in resedimented diamictite, Sapopema well core.

non-bioturbated heteroliths (lenticular, flaser and wavy bedding), massive and laminated mudstones, rhythmites, paleosol and coal (Table 1; Figs. 2, 5). Dropstone-bearing facies occur at the lower half of this unit (Fig. 2). The stones are pebble sized, composed of granite, quartzite, schist, gneiss, quartz, feldspar, and sedimentary rocks, and gradually decrease in abundance upwards. These dropstones were observed mainly in the northern sector of the area, as far as the region of the Sapopema well core (NF-09-PR).

U2 thickens southward (Fig. 3). An exception occurs in Ribeirão Novo, where U2 presents an anomalous thickness up to 90 m and seems to be filling an incised valley cut into U1. A mudstone interval at the base of U2 has its maximum thickness in the south. It gradually passes northward into heterolithic facies before it pinches out.

A total of 963 paleocurrent measurements were taken from ripple cross-lamination and cross-stratification in sandstones of U2 in Ribeirão Novo, Tomazina, Ibaiti and Teixeira Soares successions, revealing a predominant transport direction to the SW (mean direction = 215°; Figs. 2–3).

Deposits containing fossil plants, although not exclusive to U2, are important stratigraphic markers within this unit (Figs. 2–3). The paleobotanical content includes undifferentiated plant remains and well-preserved macrofossils that allowed a taxonomic identification in Tomazina, Ribeirão Novo and Teixeira Soares (Fig. 9). Most of the fossil plant intervals are associated with coal seams, which are up to 35 cm thick.

4.1.2.1. Interpretation. U2 is interpreted to have occurred in multiple depositional settings, mostly related to transitional environments, and in different positions in relation to the paleoshoreline. Glacial influence is still recognizable in basal facies of U2 as dropstone-bearing rhythmites and heteroliths. A decrease in abundance of this feature upwards is interpreted as a gradual decrease of glacial influence through time.

Dominance of fluvio-deltaic signals were recognized in the Ibaiti, Teixeira Soares and Ivaí localities, where the well-developed coarsening- and thickening-upward successions are interpreted as deltaic progradation southwestward. The association of bidirectional paleocurrents, ripples that climb upward on the lee face of larger scale bedforms, mud drapes and presence of heteroliths points to a river-dominated delta with moderate tidal influence (e.g., Willis et al., 1999; Boyd et al., 2006; Tänavsuu-Milkeviciene and Plink-Björklund, 2009; Rossi and Steel, 2016).

The basal mudstone-dominated interval stratigraphically above U1 in Ivaí, Teixeira Soares and Canoinhas was deposited under marine influence, due to the presence of elements of the *Eurydesma* fauna (Teixeira Soares; Taboada et al., 2016) and trace-fossils of marine affinity (e.g., *zoophycos* in the Ivaí well core; Knaust, 2017). These intervals are gradually overlain by shallower, sandstone-dominated associations, locally resulting in paleosol development and plant colonization, as seen in Teixeira Soares.

The Canoinhas well core shows profuse evidence of marine/tidal influence, such as mud drapes, heterolithic facies and trace-fossil assemblage of marine affinity (e.g., *Rosselia*, *Ophiomorpha*, *Bergaueria*; Knaust, 2017). The facies associations and trace-fossil assemblage are consistent with an estuarine environment. A similar environment is attributed to the Ribeirão Novo succession, but for this latter, we suggest a wave-influenced estuary setting (Table 1), due to the presence of sandstones with wave ripples (Fig. 5F), and hummocky and swaley cross-stratification (HCS/SCS) (Dashtgard et al., 2009; Wesolowski et al., 2018).

The Chemical Index of Alteration measured in Canoinhas indicates temperate climates during most of the U2 interval, passing to arid conditions close to the boundary with U3. The Ivaí and Sapopema localities show paleoclimate conditions relatively more arid in comparison to the Canoinhas locality, based on CIA values.

The dominant paleotransport southwestward observed in all localities is interpreted as the fluvial input into the basin, and the subordinate northeastward direction reflects flood tidal currents.

4.1.3. Unit 3 (U3)

This unit is 2 to 45 m thick, broadly thins southward and comprises diamictites and, subordinately, rhythmites with lonestones. U3 rests abruptly on sandstones of U2 and is bounded on top by an unconformity underlying U4 (Figs. 6J, 7A). The upper part of U3, a few meters below the contact with U4, is marked by diamictites showing distinctive features, including vertical color changes, peds, cutans and root traces.

Sedimentary facies of U3 comprise massive diamictites, rhythmites with soft-sediment deformation, stratified diamictites and diamictites with rafted blocks (Fig. 6). In general, diamictites have well-rounded to angular polymictic clasts ranging from a few millimeters to 2 m immersed in a muddy to muddy–sandy matrix (Fig. 6). Faceted, striated and polished clasts are common (Fig. 6H–I).

Rhythmites are characterized by a mm- to dm-thick intercalation of mudstones and sandstones, sharp contacts between laminae/beds and common presence of dropstones (granules to pebbles; Fig. 6E–F). The uppermost few of meters of rhythmites show multiple forms of soft-sediment deformation, as disrupted beds, folds, layer-parallel shearing, load and flame and ball-and-pillow structures (Fig. 6D).

Stratified diamictites consist of a compositional alternation of mudstone laminae and coarser layers composed of diamictite pellets (Fig. 6C, E, G). Abundant dropstones are seen deforming the underlying strata (Fig. 6C, E). Diamictites with rafted blocks are composed by matrix and blocks of rhythmites and sandstones with variable degrees of deformation (Fig. 6B). These latter are up to 100 m long and resemble the facies of the underlying U2, regarding the composition and sedimentary structures.

4.1.3.1. Interpretation. Massive diamictites can be formed by multiple processes, as a combination of settling of fines from meltwater plumes and rain-out, debris-flow, or a combination thereof (Visser, 1994; Isbell et al., 2021). Massive diamictites and facies with rafted blocks may be different parts of a continuum process of disaggregation and mixing within subaqueous mass flows. Massive varieties would be highly evolved deposits, whereas facies with less matrix and presence of rafted blocks would represent incipient to mature mass transport deposits, depending on the deformation within rafted blocks (Rodrigues et al., 2020).

Rhythmites were deposited by low-density turbidity currents (Mutti et al., 2007) and ice rafting and are immediately overlaid by mass transport diamictites. The basal interaction beneath the mass flow and the upper zone of the substrate (rhythmites) originated abundant soft-sediment deformation in this latter. Stratified diamictites of U3 involved settling of fines from meltwater plumes and coarser material (diamictite pellets and dropstones) released from iceberg rafting (Powell and Domack, 2002; Isbell et al., 2021).

4.1.4. Unit 4 (U4)

Unit 4 (U4) is the youngest interval of the studied succession and comprises clastic and organic-rich facies (Fig. 7). The basal boundary is mostly erosional, and in the northern part of the area (Ibaiti and Figueira), it is marked by a prominent subaerial unconformity associated with paleosols, incised valleys and laterally discontinuous conglomerates (Fig. 7A). This unit marks the definitive disappearance of diamictite facies and the introduction of a laterally persistent succession of medium- to coarse-grained sandstones, causing a sharp deflection to low gamma-ray values (Fig. 3).

The lower part of U4 is dominated by medium- to coarse-grained sandstones with planar and trough cross stratification, inverse grading, unidirectional or bidirectional current ripples with mud drapes, and local intercalations with conglomerates (Fig. 2). The basal sand-rich interval may be overlain by mudstone-dominated intervals, as the thick paleosol developed on mudstones in Sapopema (Fig. 7H), or alternating muddy (mudstones, heteroliths, and coal) and sandy (massive, cross-stratified) intervals, as observed in the Canoinhas, Ivaí and Ibaiti sections (Figs. 2, 7B–G).

Coal seams may rest directly on the basal unconformity of U4, along with alternating coaly and rooted mudstones and sandstones, as in the abandoned coal mine of Ibaiti, or alternatively, in the upper half of U4, like in the Canoinhas well core (Fig. 2). In Ibaiti/Figueira and Ortigueira localities, the coal seams are associated with a characteristic paleoflora (e.g., Fig. 7D).

The values of the Chemical Index of Alteration for U4 do not show significant variation across the three localities. In Canoinhas, the CIA values range from 68.2 to 68.6, in Ivaí from 62.5 to 65.9, and in Sapopema, from 65.6 to 68.8 (Fig. 8).

4.1.4.1. Interpretation. U4 was deposited mostly in tide-dominated to tide-influenced environments (Table 1). Signs of tidal reworking include bidirectional currents, reactivation surfaces, mud drapes and heterolithic facies. A tide-dominated to mixed estuarine setting was

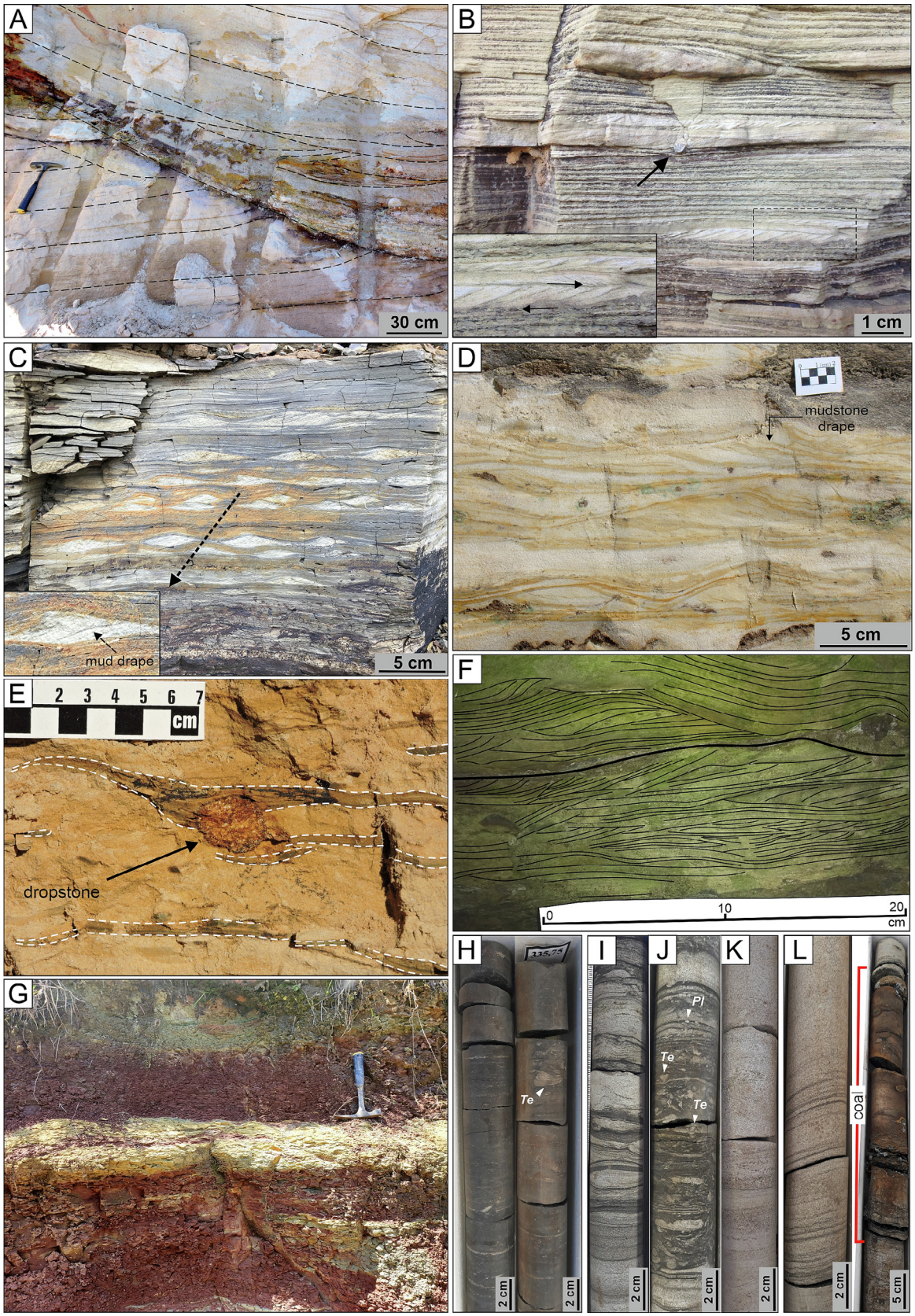

previously interpreted for this unit based on data from Ibaiti (Zacharias, 2004; Zacharias and Assine, 2005). According to these authors, sandy facies are assigned to tidal channel-fill deposits and mudstones along with coal seams were deposited in tidal mudflats. The laterally discontinuous association of conglomerates and coarse-grained sandstones was assigned to fluvial deposits, formed above the tidal influence (Zacharias, 2004).

U4 records the definitive shift to postglacial conditions, as dropstone-bearing facies and diamictites are no longer recognized. The onset of postglacial conditions is corroborated by the general increase in the chemical weathering through time in U4 (Fig. 8), suggesting climate improving. However, the Sapopema CIA profile shows an anomalous low value of chemical weathering at the base of the U4, with a posterior deflection to the right indicating climate improving.

4.2. Floral record

Three fossiliferous localities were recognized in the study area, corresponding to Tomazina, Ribeirão Novo and Teixeira Soares (Fig. 1B). The fossil plant-bearing strata occur in different facies associations and are related to coal seams in Ribeirão Novo and Teixeira Soares (Mottin, 2022).

4.2.1. Tomazina flora

Plant remains were described in an abandoned quarry aside PR-272 Highway (UTM coordinates SIRGAS2000: 604135, 7369317). The plant-bearing facies is a fine- to medium-grained massive sandstone deposited in a subaerial delta plain environment. The subaerial setting is evidenced by abundant root traces and paleosol underlying the fossiliferous bed. The macrofloristic content includes undetermined wood impressions up to 10 cm in diameter, besides impressions of *Paracalamites* sp. and leaves identified as *Gangamopteris obovata* (Fig. 9C).

4.2.2. Ribeirão Novo flora

Fossiliferous beds belonging to U2 were identified in outcrops located in the Ribeirão Novo River basin (e.g., UTM coordinates SIRGAS2000: 622822, 7363589), Wenceslau Braz county, northeast Paraná State (Fig. 1B). The identified fossil plant material was retrieved from a mudstone interval of the upper U2, a few meters below the contact with U3 (Figs. 2–3). Three lower fossil-bearing intervals contain undifferentiated plant remains (Figs. 2–3).

Elements in this flora were originally described by Guerra-Sommer et al. (1981) and, according to our re-examination, include fronds of *Botrychiopsis plantiana* (Fig. 9A, E), sphenopsid leaf branches of *Phyllotheca* cf. *P. australis* (Fig. 9B, D) and stems of *Paracalamites* sp. (Fig. 9D), besides seeds classified as *Cordaicarpus* sp. (Fig. 9F).

4.2.3. Teixeira Soares flora

The most important fossiliferous outcrop in Teixeira Soares is located in the stream banks of the Córrego do Minhocão (UTM coordinates SIRGAS2000: 553907, 7198789). The fossil plant-bearing mudstones represent floodplain deposits of a coastal plain environment (Table 1), associated with accumulation of organic matter (coal seam). The interval is positioned in the upper third of U2, interbedded with decametric cross-stratified sandstone packages, which are interpreted as fluvial channel-fill deposits.

According to the literature, the floral record of Teixeira Soares comprises common leaf impressions of glossopterids and few remains of sphenopsids and conifer shoots. Oliveira (1927) was the pioneer in the collection of plant fossils in this locality, having identified distinct species of glossopterid leaves, i.e., *Glossopteris* (=*Gangamopteris*?) *obovata*, *G. browniana*, *G. indica* and *G. occidentalis*, besides leafy branches of sphenopsids, i.e., *Phyllotheca* sp., and from conifers, i.e., *Voltzia* sp., and a type of seed, i.e., *Cardiocarpum* (=*Cordaicarpus*) *seixasi*. Afterwards, Read (1941) confirmed the occurrence of *G. browniana*, rejected the presence of *Glossopteris obovata* and *G. occidentalis*, and reclassified *Voltzia* sp. into *Brachyphyllum* cf. *australe*. In turn, Almeida (1945) added the presence of a possible whorl of *Sphenophyllum* in the flora of Teixeira Soares. Finally, Dolianiti (1948) reclassified *Brachyphyllum* cf. *australe* into *Paranocladus*? *fallax* and afterwards he indicated the occurrence of *Glossopteris orbicularis* in this locality (Dolianiti, 1954).

Recently, some of authors (TEM, FFV, RI) recovered abundant impressions of *Paracalamites*-like sphenopsid stems from the same phytofossiliferous bed worked by Oliveira (1927) and Almeida (1945). Furthermore, during the review of the material from Teixeira Soares published by Oliveira (1927), we noticed a specimen arranged in the upper left corner of a plate (in between pages 52 and 53) that clearly corresponds to a frond fragment of a fern that supports pecopterid pinnules. This occurrence will be named here as *Pecopteris* sp.

Therefore, the updated plant association of Teixeira Soares is as follows:

Paracalamites sp.
Phyllotheca sp.
Sphenophyllum sp.
Pecopteris sp.
Glossopteris browniana
Glossopteris indica
Glossopteris orbicularis
Paranocladus? *fallax*.

5. Discussion

5.1. Depositional history

The interval comprised by U1 to U4 represents the stacking of two consecutive deglaciation cycles (U1 and U3) interspersed with an interglacial stage (U2), assigned to the Taciba Formation (upper Itararé Group), and the onset of postglacial conditions (U4) ascribed to the lower–middle Rio Bonito Formation (Mottin, 2022). We did not find evidence of subglacial erosion/deformation/deposition associated with U1 and U3, but the presence of dropstones, diamictite pellets, faceted, striated, and oversized clasts of exotic composition within mass-flow diamictites supports subaqueous deposition associated with a retreating ice margin (Mottin et al., 2018; Isbell et al., 2021). Glacially-influenced sequences consisting mostly of deglaciation products, like those of U1 and U3, are not uncommon (e.g., Martini and Brookfield, 1995; Visser, 1997; Kneller et al., 2004) and in most basins they form the bulk of the sedimentary record of a glaciation.

The evolutionary history of the study interval begins with deposition of diamictites of U1 in a first episode of deglaciation. Previous studies in the Ibaiti region recognized algal species of marine affinity in diamictites belonging to U1, denoting thus deposition in a glaciomarine environment (Mottin et al., 2018, 2020).

Deposition of U2 gradually ensued the first deglaciation represented by U1, which is corroborated by the presence of dropstones at the base of U2 and their decrease upwards, marking the progressive decline of

Fig. 5. U2. (A) Large scale trough cross stratification in coarse-grained sandstone characteristic of a tide-influenced delta plain in Ibaiti-PR. (B) Sandy rhythmite with bidirectional paleocurrents ascribed to a tide-influenced delta front environment in Ibaiti. (C) Heterolith showing lenticular bedding and mud drapes in ripple foresets, Tomazina-PR. (D) Asymmetrical to symmetrical mud-draped ripples in fine-grained sandstones, Ribeirão Novo. (E) Dropstone-bearing heterolith (flaser bedding) in Ibaiti, interpreted as a tide-influenced delta front deposit. (F) Shoreface sandstone exhibiting wave ripples in Ribeirão Novo. (G) Metric mudstone interval assigned to a flood plain environment, Teixeira Soares-PR. (H) Weakly bioturbated black shale ascribed to a prodelta/marine offshore environment, base of the Canoinhas well core. (I) Heterolithic facies of the Canoinhas well core showing soft-sediment deformation and medium degree of bioturbation. (J) Coal bed in estuarine facies association of the Canoinhas well core. Abbreviations: *Te* = *Teichichnus*, *Pl* = *Planolites*.

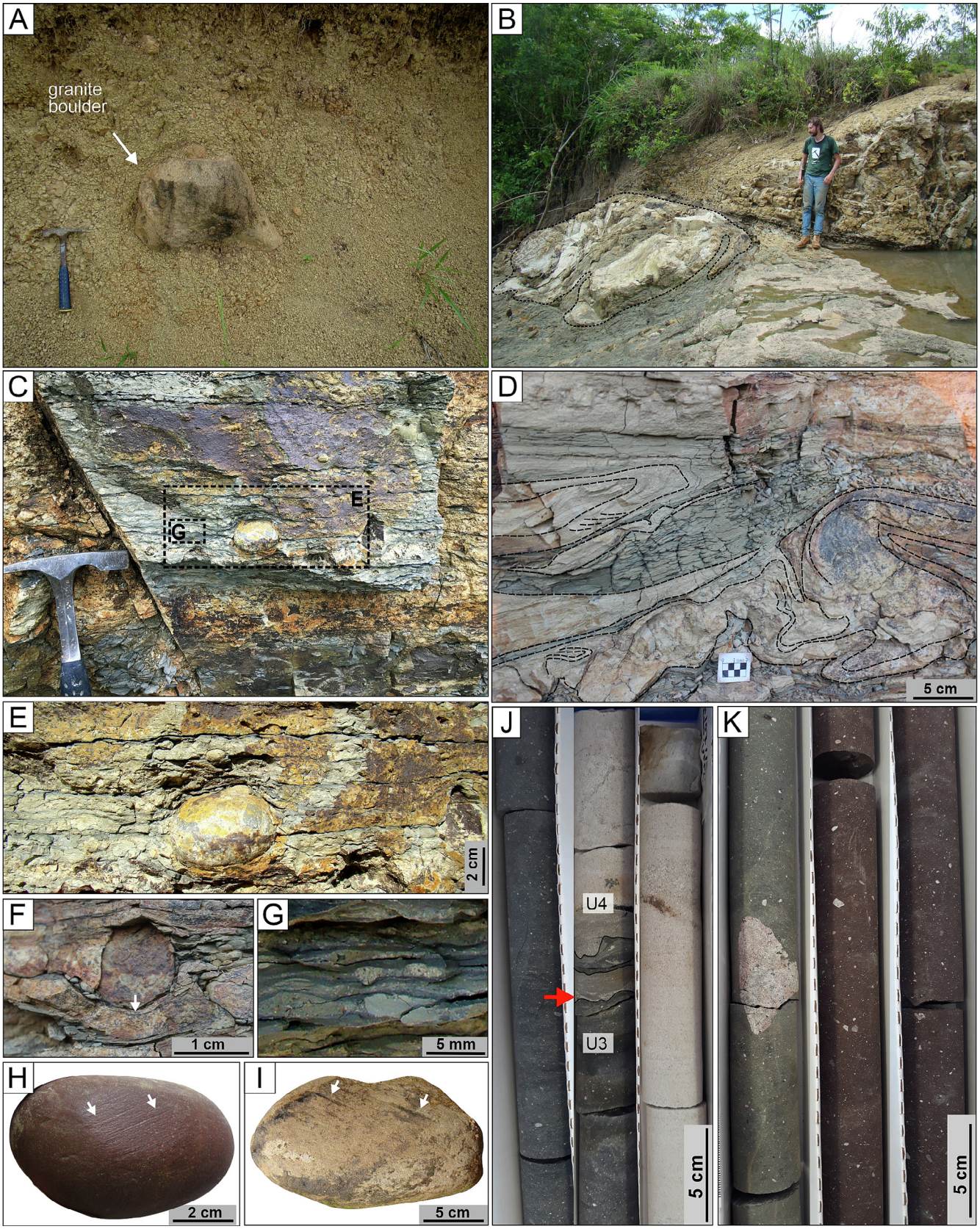

Fig. 6. U3. (A) Massive diamictite displaying an angular granitic boulder in Ibaiti. (B) Deformed metric rafted block of sandstone within a resedimented diamictite of U3 exposed in Ibaiti. (C) Muddy and diamictite pellet layers arranged in successive laminae in stratified diamictite in Tomazina. Note rounded dropstone in the center. (D) Synsedimentary deformation (recumbent folds, load casts) affecting dropstone-bearing rhythmite in Ribeirão Novo. (E) Enlarged view of dropstone seen in C. (F) Dropstone deforming rhythmite laminae of U3 in Ribeirão Novo (G) Enlarged view of C, showing lenticular diamictite pellets deforming muddy laminae. (H–I) Well-rounded, faceted and striated clasts retrieved from diamictites of U3. (J) Erosive contact between U3 (dark gray diamictite) and U4 (white sandstone) and (K) angular granite granules and pebbles immersed in massive diamictite of U3, both from the Ivaí well core.

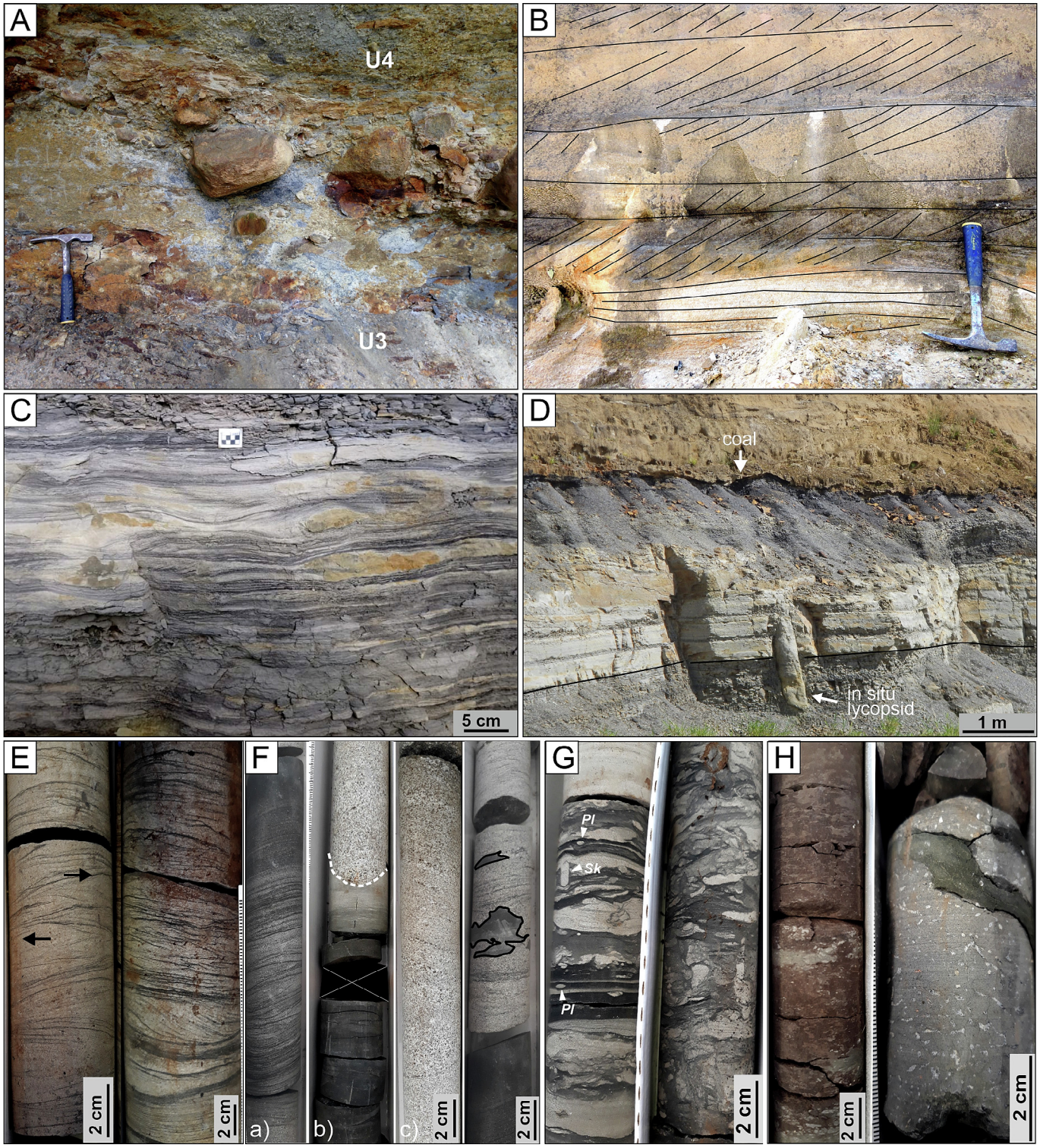

Fig. 7. U4. (A) Contact between U3 and U4 in Ibaiti, marked by a conglomeratic level with boulders of crystalline rocks. (B) Shallow marine, coarse-grained sandstone showing planar-parallel lamination and tangential cross-stratification in Ortigueira. (C) Lenticular bedding passing to wavy bedding in Ortigueira. (D) Upright lycopsid cast cropping out in the Ortigueira locality. The host succession comprises sandstones, mudstones, heteroliths and coal. (E) Flaser heterolith with bidirectional ripples and mud drapes, Canoinhas well core. (F) a) Flaser bedding exhibiting double mud drapes, b) erosive contact of laminated mudstone and stratified coarse-grained sandstone, c) cross-stratified, coarse-grained and immature sandstone, and d) black mud rip-up clasts dispersed in coarse-grained sandstone overlying black mudstone in the Ivaí well core. (G) Moderately to intensely bioturbated heteroliths in the Ortigueira well core (FP-05-PR). (H) Paleosols developed on mudstones in the Sapopema well core, showing mottling features (left) and calcic horizon, where carbonates are the white spots (right). Abbreviations: *Pl* = *Planolites*, *Sk* = *Skolithos*.

the glacial influence. This process ultimately culminated with the development of ice-free depositional systems (Table 1), characterized by relatively dense vegetation, soil formation and coal accumulation, that is ultimately interpreted as an interglacial stage, indicating significant climate improvement after deglaciation. Moderate to high values of CIA in U2 are comparably slightly lower to those of postglacial deposits of U4 and indicate temperate paleoclimates (Fig. 8).

An up to 35 m thick interval of dropstone-free siltstones and shales at the base of U2, observed as high gamma-ray responses, and informally named as "Passinho Shale" (Almeida, 1945; Lange, 1954),

Table 1
Summary of the main characteristics and interpretations regarding the four units recognized in outcrops and well cores.

Unit	Depositional system	Facies association	Sedimentary facies	Thickness	Fossil content	Interpretation
U1	Glaciomarine	Resedimented diamictites	Massive diamictite with angular to rounded outsized clasts immersed in a silty to sandy–muddy matrix. Clasts range from granule to boulder (max. size: 1.2 m), are commonly faceted, striated and bullet-shaped	5–15 m	N/O	Debris rain-out (mud, sand and oversized clasts), and/or resedimentation of glacial material through subaqueous debris flows, or a combination thereof (e.g., Gama Jr. et al., 1992; Eyles et al., 1993; Visser, 1989, 1994)
			Diamictite matrix characterized by mm- to cm-thick textural bands (muddy and sandy discontinuous layers) and dispersed granules to pebbles. Presence of intrabasinal blocks and abundant soft sediment deformation structures. Presence of scattered dropstones		N/O	Resedimentation of bedded sediment via subaqueous slumping, producing synsedimentary deformations and remobilization of intrabasinal blocks of outwash deposits (Mottin et al., 2018). Presence of dropstones indicates iceberg rafting prior the resedimentation
			Diamictites with a sandy–muddy homogeneous matrix and undeformed to highly-deformed intrabasinal blocks (rafts) of sandstones and conglomerates. Blocks may exhibit internal deformation including folds and faults		N/O	Deposition in a subaqueous setting by mass-gravity flow, involving remobilization of outwash sandstones and conglomerates via slumps (e.g., Shanmugam, 2006; Posamentier and Martinsen, 2011; Mottin et al., 2018; Rodrigues et al., 2020)
U2	Relatively deep-water	Prodelta/bay	Massive, dropstone-bearing and bioturbated mudstones; lenticular, wavy and flaser bedding with bioturbation	A few cm to 18 m	*Teichichnus*, *Planolites*; *Eurydesma* fauna[a]	Fine-grained pelagic fallout combined with deposition of ice-rafted debris from floating ice.
	Delta-front	Tide-influenced delta front	Coarsening- and thickening-upward successions of muddy and sandy rippled rhythmites with foreset dip reversals and mud drapes; intercalation of massive rhythmites and dm- to m-thick tabular structureless sandstones; lenticular and flaser bedding. Dropstones decrease in abundance upwards	19 m	*Helminthoidichnites tenuis*	Rhythmites: interpreted as thin-bedded turbidites deposited by low-density turbidity currents. Frequent tidal influence in Ibaiti, evidenced by bidirectional paleoccurrents and mud drapes. Dropstones introduced by floating ice. Thick-bedded and structureless sandstones: deposited by high-density turbidity currents (c.f., Lowe, 1982)
		Delta front failure	Dropstone-bearing heteroliths with recumbent and sheath folds, compositional banding homogenization, normal and reverse faults, clay smear	13 m	N/O	Sharp-based sandstone beds with abundant mud rip-up clasts alternating with thinner mudstone units are typical deposits of turbidite flows (Mutti et al., 2007). Evidence of tidal influence point to original deposition in a delta front environment. Deformational structures suggest final deposition by slumping (Shanmugam, 2006; Posamentier and Martinsen, 2011)
		Tide-influenced lower delta front, mouth bar	Upward-coarsening succession of intensely bioturbated heteroliths (lenticular, wavy and flaser bedding), massive, planar-parallel and planar cross-stratified, medium- to coarse-grained sandstones. Upward increase in sedimentary structure scale	Up to 24 m	*Zoophycos*, *Planolites*, *Thalassinoides*, *Teichichnus*, *Diplocraterion*	Lenticular, wavy and flaser bedding facies represent distal parts of the mouth bar, formed by alternating bedload transport and suspension fallout. The gradual upward increase in sandstone facies and size of the sedimentary structures indicates a delta front progradation (mouth bar). Flaser bedding, mud drapes and current reversals attest to tidal reworking
	Coastal to shallow-water	Delta plain/tide-influenced delta plain	Sandstones with trough and planar cross-stratification, massive structure, horizontal lamination and ripple cross-lamination; paleosol, coal	1.5–10 m	*Gangamopteris obovata* and wood fragments	Deposits of fluvial channel-fill in a subaqueous to subaerial environment, this latter supported by the presence of paleosol and rooted mudstones
		Wave-dominated estuary (lagoon, shoreface)	Shoreface: sandstones with hummocky (HCS) and swaley cross-stratification (SCS), current and wave ripples, horizontal lamination, trough and planar cross-stratification, soft-sediment deformation	10–80 m	*Eurydesma* fauna[a]	HCS and SCS record the action of high energy, oscillatory and combined flows and are interpreted as shoreface storm deposits. Current and wave ripples and parallel lamination intercalated with HCS and SCS facies indicate periods of low intensity of storms and action of oscillatory (fair-weather waves) and unidirectional flows (Wesolowski et al., 2018)
			Lagoon: plant-bearing mudstone; laminated and massive sandstones; coal. Pervasively rooted interval (roots up to 8 cm deep) precedes the coal bed	15 m	*Botrychiopsis plantiana*, *Phyllotheca* sp., *Paracalamites* sp., *Cordaicarpus* sp.	Suspension fallout under quiet water setting, followed by a relatively higher energy setting later colonized by plants, and accumulation of plant debris in a swamp, oxygen deficient environment
		Coastal plain	Fluvial channel: alternation of conglomerates, medium- to coarse-grained massive sandstones, planar-parallel lamination and trough cross-stratification	40 m	N/O	Sandstone and conglomerate facies represent the infilling of fluvial channels
			Floodplain: Massive siltstones, fossil-plant bearing and coaly mudstones, coal, paleosol		*Gangamopteris obovata*, *Phyllotheca australis*, *Phyllotheca* sp., *Paracalamites* sp., *Pecopteris* sp., *Sphenophyllum* sp., *Glossopteris browniana*, *Glossopteris indica*, *Glossopteris orbicularis*, *Paranocladus*? *fallax*[c]	Coaly and plant-bearing mudstones are associated with aggradation in a vegetated floodplain environment. Coal formed by accumulation of organic matter in reducing environment. Paleosols are indicative of subaerial exposure, intemperism and colonization by plants

		Tide-dominated estuary	Tidal channel: coarse-grained and immature sandstones with basal lag and interbedded conglomeratic layers, planar cross stratification and horizontal lamination. Presence of subhorizontal mud films and mud/intraclast drapes in cross-stratified sandstones	4–10 m	N/O	Sandstones with erosional basal contacts and conglomeratic lags are interpreted as estuary channel-fill deposits. Stratified sandstones suggest migration of subaqueous dunes alternated with deposition of mud and intraclasts on dune foreset during slack water period
			Lower tidal mud flat and tidal creeks: highly bioturbated lenticular, wavy and flaser bedding, rhythmites, massive mudstones and sandstones, rippled sandstones with mud drapes, mudstones with soft-sediment deformation, coal	8–29 m	*Teichichnus*, *Planolites*, *Rosselia*, *Ophiomorpha*, *Thalassinoides*, *Lockeia*, *Scolicia*, *Arenicolites*, *Cylindrichnus*, *Diplocraterion*, *Bergaueria*, *Skolithos*, scape trace	Lenticular, wavy and flaser bedding records alternating bedload transport during tidal flow and suspension fallout during slack water periods (e.g., Buatois et al., 1999)
U3	Glaciomarine	Turbidites	Rhythmites characterized by mm- to dam-thick intercalation of mudstones and rippled/massive sandstones and common lonestones/dropstones. Presence of soft-sediment deformation in the form of abundant folds, faults, ball-and-pillow and load structures	2–45 m	N/O	Rhythmites were deposited by low-density turbidity currents along with ice rafting and are overlaid by mass transport diamictites. Deformation of the superior part of the rhythmite succession may be related to the basal interaction of the mass flow (diamictite) and the unlithified substrate (rhythmite), by means strain transmission from the flow into the upper zone of the substrate (Sobiesiak et al., 2018)
		Rain-out diamictites	Pebbly diamictite characterized by a muddy matrix pierced by abundant dropstones and diamictite pellets, arranged in successive laminae sets, forming horizontal stratification.		N/O	Settling of fines from meltwater plumes forming the muddy laminae and coarser material (diamictite pellets and dropstones) released from iceberg rafting (Powell and Domack, 2002; Isbell et al., 2021)
		Resedimented diamictites	Sandy–muddy diamictites holding dam-scale intrabasinal blocks of rhythmites and sandstones. Blocks and matrix may exhibit synsedimentary deformations including folds, faults, shear planes, boudins		N/O	Deposition in a subaqueous setting by mass-gravity flows, involving remobilization of deltaic rhythmites and sandstones of U2 via slumping (e.g., Shanmugam, 2006; Posamentier and Martinsen, 2011; Rodrigues et al., 2020)
U4	Coastal to shallow-water	Tide-dominated to mixed estuary - Tidal channel and tidal mudflats[b]	Fine-grained sandstones with symmetrical and asymmetrical ripples; medium- to coarse-grained sandstones with planar, trough and sigmoidal cross-stratification; asymmetrical ripples, horizontal lamination and massive structure	Up to 24 m	*Pecopteris* spp., *Asterotheca derbyi*, *Sphenophyllum brasiliensis*, *Annularia* spp., *Brasilodendron* sp., *Paranocladus* spp., *Buriadia figueirensis*, *Glossopteris* spp., *Gangamopteris obovata*, *Paranospermum cambuiense*[d]	Deposition in tidal/fluvial channels. Tidal influence is suggested by mud drapes on foreset of cross-strata. Unimodal transport indicates dominance of fluvial and/or ebb tide currents
			Massive and laminated mudstones, organic-rich shales, discontinuous coal beds			Represent deposits of a low energy, tide-dominated/influenced environment as tidal mudflats of a tide-dominated or mixed estuary
		Tide-influenced delta	Laminated, massive and rooted mudstones, cross-stratified, massive, rippled (bidirectional), laminated and soft-sediment deformed fine sandstones, coaly mudstones and coal		*Brasilodendron*-like lycopsid, *Paracalamites* sp., *Pecopteris* sp.[e]	Massive and rooted mudstones represent deposition in interdistributary zones of a lower delta plain. Fine-grained sandstone facies resulted from deposition of crevasse-splay subdeltas (e.g., Gugliotta et al., 2015). Coaly mudstones and coal represent sedimentation in vegetated distal parts of the crevasse splay
		Tide-dominated estuary	Rippled sandstones with current reversal and mud drapes, planar cross-stratified sandstone, flaser and lenticular bedding, massive and bioturbated mudstones, coal	22 m	Undifferentiated plant remains; horizontal excavations	Mudstones, heterolithics and coal were deposited on tidal flats, whereas stratified/laminated sandstones with mud drapes represent tidal channel deposits
		Estuary	Tidal channel: planar cross-stratified sandstone locally with organic-rich drapes, massive sandstones with mud rip-up clasts, mud films and scoured top	15 m	N/O	Migration of subaqueous dunes in a tidal channel setting. Bidirectional currents, organic-rich drapes and mud films point to tidal rework
			Tidal flat: flaser bedding, massive mudstones commonly infilling scours at the top of sandstone beds			Alternating bedload transport during tidal flow and suspension fallout during slack water periods (e.g., Nio and Yang, 1991; Buatois et al., 1999)
			Sandstones with current ripples and mud drapes, horizontal lamination and massive structure, lenticular bedding, paleosol	26 m	N/O	Sandstone facies with evidence of tidal rework represent tidal channel-fill deposits. Mudstones, heteroliths and paleosol suggests deposition in a tidal flat environment

[a] According to Neves et al. (2014a, 2014b) and Taboada et al. (2016).
[b] According to Zacharias (2004).
[c] According to Oliveira (1927) and this study.
[d] According to Ricardi-Branco (1997) and Iannuzzi et al. (2010).
[e] According to Mottin et al. (2022).

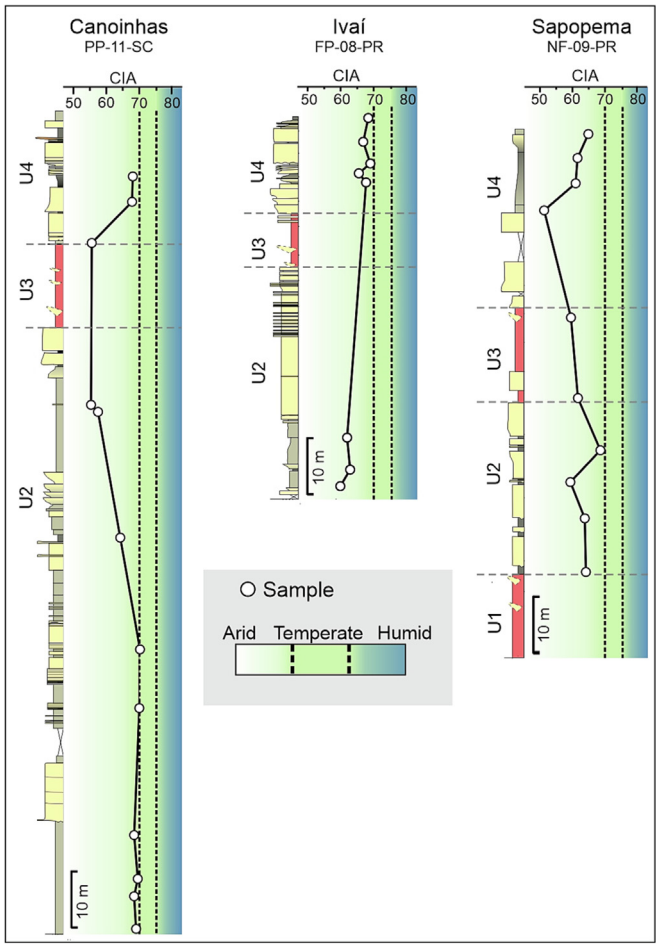

Fig. 8. Stratigraphic sections of Canoinhas, Ivaí and Sapopema well cores and their respective variations of the CIA values through time. Units are delimited by gray lines.

overlaps the diamictites of U1 between the Cândido de Abreu and Canoinhas cores (Fig. 3). It gradually increases in thickness southward, following the thickening direction of U2. The "Passinho Shale" represents a widespread transgression event in the basin, here interpreted as having been driven by the first deglaciation event.

Different stacking patterns characterize U2 across the study area. The southern sections show a pronounced transgressive trend at the base ("Passinho Shale"), abruptly passing to a shallowing-upward trend (sharp-based motifs in Fig. 3). The "Passinho Shale" is not recorded in the northern part of the area, where U1 is directly overlaid by shallow-marine to coastal facies associations of U2 (Table 1; Fig. 3), also displaying a shallowing-upward pattern.

These contrasting patterns probably result from the relative positioning of the two extremes of the study area in relation to the retreating ice-margin. The southern extreme represents distal marine sedimentation, defining a transgression, as a direct consequence of eustatic sea-level rise that followed the first deglaciation (U1). Sequences similar to this are characteristic of eustatically-dominated zones by Boulton (1990). The opposite (northern) extreme, more closely resembles deposition in isostatically-dominated zones (Boulton, 1990), where the interglacial phase is represented by regressive successions (e.g., Nutz et al., 2015; Dietrich et al., 2017).

Coastal to shallow-marine facies associations at the top of U2 (Table 1; Figs. 2–3) are sharply capped by mud-rich diamictites and dropstone-bearing rhythmites of U3, causing an increase in gamma-ray values (Fig. 3). The accommodation of tens of meter thick resedimented deposits assigned to deeper environments, necessarily implies an increase in water depth. Presence of dropstones, diamictite pellets and glacially transported clasts in deposits of U3 suggests the occurrence of a second glacial pulse, which was likely responsible for this change in the base level. Isostatic depression of the crust can cause this increase in the water depth if the period of ice loading is adequate to produce the necessary marine submergence (Boulton, 1990; Visser, 1993).

The contact between U3 and U4 is an unconformity in the northern part of the area (Fig. 7A), which is evidenced by a thick paleosol developed from diamictites of the uppermost U3 (Mottin et al., 2018; Mottin and Vesely, 2021) that is laterally associated with NE–SW oriented incised valleys (Zacharias and Assine, 2005). These valleys are filled by estuarine facies and have coal seams on the interfluves (Zacharias and Assine, 2005), corresponding to U4. The contact passes from subaerial to subaqueous southward, indicated by soft-sediment deformations at the boundary between diamictites of U3 and estuarine sandstones of U4 (e.g., Fig. 6J).

The origin of the subaerial unconformity and the forced regressive deposits of U4, i.e., lower Rio Bonito Formation, that sharply overlain the mass-transport diamictites of U3, were assigned by Zacharias and Assine (2005) to the isostatic rebound associated with the end of the late Paleozoic glaciation in this part of the basin. This process would have led to the uplift of the northern part of the Paraná Basin, increase in erosion and formation of a sequence boundary (e.g., Boulton, 1990; Lambeck, 1991; Dietrich et al., 2017).

U4 is also represented by different stacking patterns along the area, resembling U2. The interpreted paleoenvironments range from alluvial plains to estuaries. We interpret this lateral variability as a response to the general paleogeography of the basin, similarly to U2, and/or distinct configurations of the shoreline, where different and coeval depositional systems may occur side by side. As for the chemical weathering, U4 in general shows increasing values of CIA upwards, and the range of those values corresponds to temperate conditions. An anomalously low value of the index is observed at the base of U4 in Sapopema, indicating arid conditions. Additional analysis such as petrography and XRD could reveal whether the value was controlled by geological factors (e.g., hydrodynamic sorting, source rock composition), instead of the paleoclimate.

5.2. Paleogeographic outcomes

Multiple lines of evidence exposed herein suggest that the sediment dispersal pattern in the studied interval differs from the lower levels of the Itararé Group. The Lagoa Azul and Campo Mourão formations, basal and middle units of the Itararé Group, respectively, show paleo ice flow and sediment dispersal from south/southeast to north/northwest in the Paraná State (Vesely and Assine, 2004, 2006; Vesely et al., 2015; Carvalho and Vesely, 2017; Rosa et al., 2019).

The fact U2 thickens southward and that the "Passinho Shale" pinches out to the north corroborates the location of the depocenter, and then the sediment transport direction southwestward of the Taciba Formation, observed in all the studied localities (Fig. 3; Mottin, 2022). The interpretation of a depocenter to the southwest is also corroborated by the predominant southwestward sediment transport direction during the deposition of the lower Rio Bonito Formation, as observed in the northeastern region of the Paraná State (see also Zacharias, 2004; Zacharias and Assine, 2005).

Moreover, diamictites of U1 and U3 thin southward, and the latter even tends to disappear farther south (Fig. 3), suggesting that the general direction of gravity flows was toward south/southwest and that a glacial source was somewhere farther north. Paleo-mass transport to the south in the Taciba Formation has been also supported by multiple statistical methods applied to different deformation structures (Rodrigues et al., 2021).

Accordingly, the final glaciation (U3) seems to have reached only the northeastern domain of the Paraná Basin. The record of glacial influence in the interglacial interval (U2), in the form of dropstones, supports this interpretation, since they are present only in the northernmost sector of the Paraná State. In the São Paulo State, coal- and fossil plant-bearing

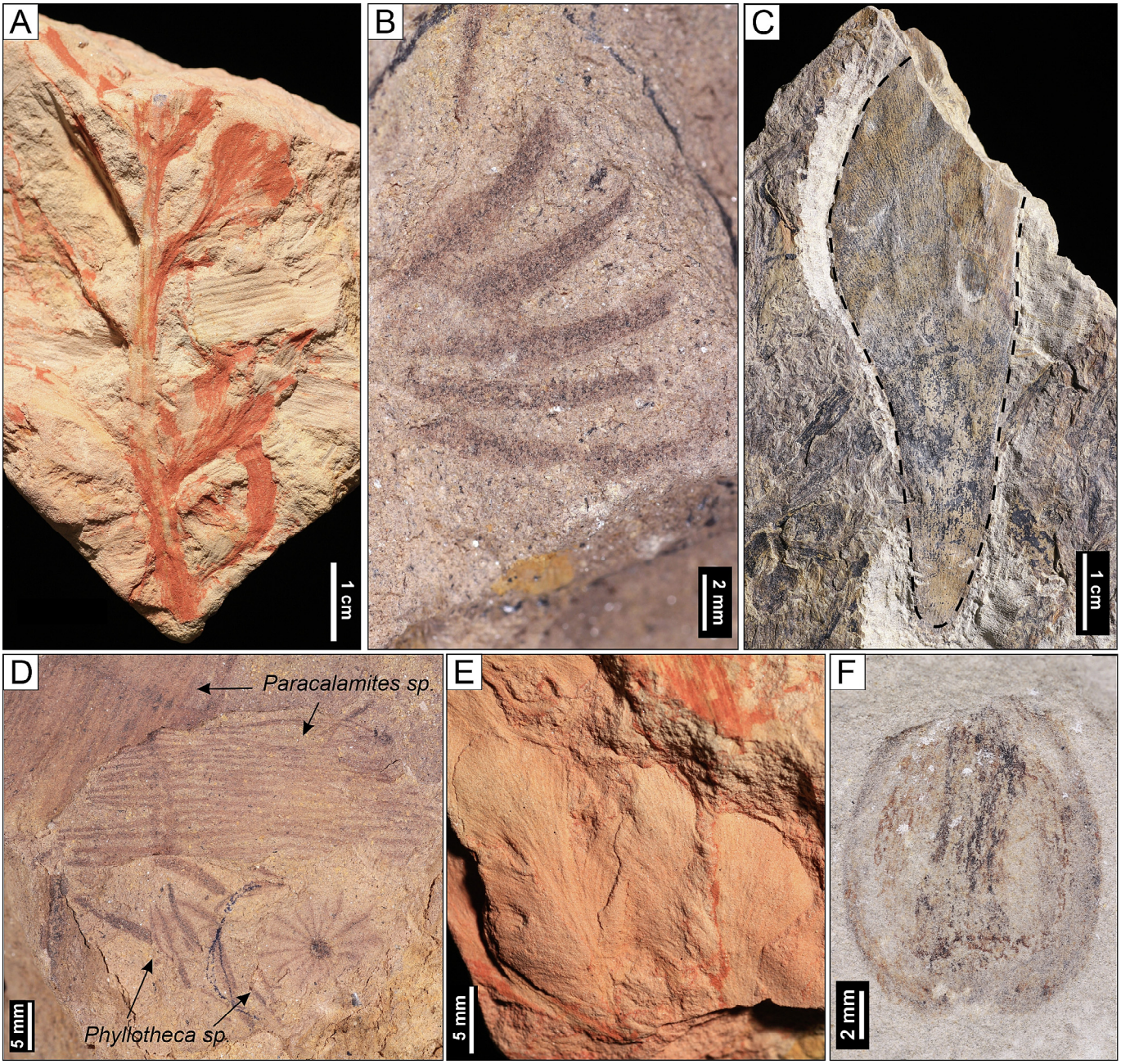

Fig. 9. Fossil plants described in deposits of U2. (A, E) Botrychiopsis plantiana. (B) Phyllotheca sp. (C) Gangamopteris obovata (D) Phyllotheca cf. *P. australis* and Paracalamites sp. (F) Cordaicarpus sp. Localities: A–B, D–F - Ribeirão Novo; C - Tomazina.

deposits similar to U2 also occur below a diamictite interval in Cerquilho and Tietê localities (e.g., Soares et al., 1977; Rohn et al., 2000; Bernardes-de-Oliveira et al., 2016), indicating that U3 extends laterally for at least 200 km northeastward.

Conversely, deposits assigned to the uppermost Itararé Group occurring southward of the study area (Santa Catarina State) show different paleotransport directions, mostly toward NW (e.g., Puigdomenech et al., 2015; Fallgatter and Paim, 2019; Schemiko et al., 2019; Valdez Buso et al., 2019). The divergence of paleotransport directions between these areas, in addition to the thinning of the glacially-influenced diamictites of U1 and U3 southward implies a glaciated source area located northwest of the Paraná State. This hypothetical glaciated area diverges from the long-proposed glacial-sources for the Paraná Basin that entered the basin on its southern margin (e.g., França and Potter, 1988; Santos et al., 1996; Vesely and Assine, 2006; Rosa et al., 2016).

5.3. Insights from the fossiliferous record into the timing of glaciation and glacial–postglacial transition

5.3.1. Flora

Deposits of U2 record a still poorly documented and stratigraphically disputable paleoflora in Tomazina, Ribeirão Novo and Teixeira Soares localities (Mottin, 2022). *Botrychiopsis plantiana*, *Phyllotheca* cf. *P. australis* and *Gangamopteris obovata* are characteristic taxa retrieved from U2 in Ribeirão Novo and Tomazina. These taxa also have been reported for other areas of the Paraná Basin (Table 2), as in the São Paulo State (i.e., Cerquilho and Tietê; Bernardes-de-Oliveira et al., 2016) and Rio Grande do Sul State (i.e., lower part of Morro do Papaleo, Candiota and Quitéria; Jasper et al., 2003; Iannuzzi et al., 2007a, 2007b), besides the Paganzo Basin in west Argentina, in the Bajo de Veliz Formation (Fernández, 2021; Fig. 1A).

Table 2
Key-taxa present in distinct phytofossiliferous localities associated to the *Phyllotheca–Gangamopteris* Flora, in the Paraná Basin, and Gangamopteris Flora, in the Paganzo Basin. All of those are considered as earliest Permian in age. Legend: X = presence; cf. = presence of the species to be confirmed.

Taxa	Paganzo Basin	Paraná Basin						
		Rio Grande do Sul			Paraná		São Paulo	
	Bajo de Veliz	Candiota	Quitéria	Morro do Papaléo (lower)	Tomazina	Ribeirão Novo	Tietê	Cerquilho
Botrychiopsis plantiana	X	X	X	X		X		
Stephanophyllites sanpaulensis	X		X	X				X
Gangamopteris obovata	X	X		X	X		X	X
G. buriadica	X		X	X			X	X
Cheirophyllum speculare	X			X				
Phyllotheca australis	X		X	X		cf.	X	X
Arberia minasica	X		X	X			X	X
Arberiopsis			X					X
Giridia	X		X					X
Lycopodites		X	X					X
Coricladus		X	X					
Rhodeopteridium			X	X				

This flora in the Paraná Basin corresponds to the *Phyllotheca–Gangamopteris* (P–G) Flora of Iannuzzi and Souza (2005). The P–G Flora is characterized by the dominance of *Phyllotheca*-type sphenophytes and *Gangamopteris* leaves, low diversity of *Glossopteris* leaves and absence of true ferns (pecopterids and sphenopterids) and sphenophyllaleans (Iannuzzi and Souza, 2005; Iannuzzi et al., 2007a; Iannuzzi, 2010, 2021). *Botrychiopsis plantiana* and *Stephanophyllites sanpaulensis* are considered guide-species, as they are exclusive to the P–G Flora. These taxa are also present in the Bajo de Véliz Formation (Fig. 1A; Table 2), supporting the establishment of a biostratigraphic correlation with the easternmost portion of the Paganzo Basin. Recently, Fernández (2021) highlighted the biostratigraphic importance of *B. plantiana* as an index taxon for the Carboniferous–Permian transition in western Gondwana.

Strata bearing the P–G Flora represent a well constrained time span, as suggested by high precision U–Pb CA-TIMS ages of ash falls in Quitéria and tonsteins in Candiota, both associated with the P–G Flora (Iannuzzi et al., 2007b; Iannuzzi, 2010). These localities present mean ages of approx. 298 Ma (earliest Asselian; Griffis et al., 2018) and are assigned to the postglacial Rio Bonito Formation. In the study area, the P–G Flora occurs within U2, and is limited at the base and top by diamictites representing glacial intervals. Therefore, the younger glaciation (U3) is not recorded in Rio Grande do Sul, as no glacial evidence occurs stratigraphically above beds containing fossil plants of the P–G Flora. The Bajo de Véliz plant assemblage is attributed to the *Gangamopteris* Flora, to which an earliest Cisuralian age is given based on correlations with other South American assemblages and other fossil groups (Fernández and César, 2019).

The plant association of Teixeira Soares is, in turn, distinct from the Tomazina and Ribeirão Novo floras. It contains a certain variety of *Glossopteris* leaf types, putative whorls of *Sphenophyllum* and fragmented fronds of *Pecopteris* (Oliveira, 1927, Read, 1941; Almeida, 1945; this study). Furthermore, no *Botrychiopsis* fronds or *Gangamopteris* leaves are present. This floristic composition corresponds to that found in the *Glossopteris–Brasilodendron* (G–B) Flora of Iannuzzi and Souza (2005). The G–B Flora is characterized by the dominance of *Glossopteris* over *Gangamopteris* leaves, either in abundance and diversity, by the frequent presence of the lycopsid *Brasilodendron* (especially in peat-forming environments) and by the emergence of sphenophyllaleans, pecopterid and sphenopterid ferns, as well as the total disappearance of *Botrychiopsis* fronds (Iannuzzi and Souza, 2005). Still, this flora is typically recorded in several localities of the Rio Bonito Formation throughout the basin, such as Morro do Papaléo and Faxinal Mine, in Rio Grande do Sul (Iannuzzi et al., 2010), different outcrops in municipalities of Criciúma, Treviso, Lauro Müller, and Rio da Estiva, in Santa Catarina (Rigby, 1972; Iannuzzi, 2010; Tybusch et al., 2012), and localities in São João do Triunfo, Figueira and Ortigueira, in the Paraná State (Figs. 1B, 3; Rösler, 1978; Ricardi-Branco, 1997, 2004; Iannuzzi, 2010; Mottin et al., 2022). Considering the record of Teixeira Soares, the G–B Flora is for the first time assigned to the uppermost portion of the Itararé Group.

Based on two high precision U–Pb radiometric ages of tonsteins in Recreio (approx. 290 Ma) and Faxinal (approx. 285 Ma) mines from the Rio Grande do Sul State, the G–B Flora spans from the latest Sakmarian to middle-Artinskian (Griffis et al., 2018, 2019a). However, the record of the G–B Flora in Teixeira Soares extends its occurrence to the latest Asselian, once it overlies a continuous section containing the middle Asselian-aged "*Eurydesma* fauna" (see next item).

Considering that the P–G Flora is older than the G–B Flora and that the latter is immediately above the *Eurydesma* fauna (Fig. 3), it is concluded that the P–G Flora is stratigraphically positioned below this transgressive event (Fig. 11). In fact, the radiometric ages obtained for the record of the P–G Flora south of the basin, in Candiota and Quitéria, i.e., 297–298 Ma (Griffis et al., 2018), are older than that obtained for the South African shales related to Eurydesma fauna in South Africa, i.e., 296 Ma (Griffis et al., 2019a), which corroborates the positioning of this flora below the Eurydesma fauna record.

Therefore, the northern sections, from Sapopema toward the north, in which taxa related to the P–G Flora appear and the Passinho Shale is not present, would represent sediments deposited before the Passinho Shale (Fig. 3). In the section of Teixeira Soares, where the Passinho Shale is present, the G–B Flora appears in the terrestrial deposits overlying the marine sediments.

5.3.2. Fauna

In the Teixeira Soares region, heterolithic strata interpreted as shoreface deposits beneath the Passinho Shale are characterized by occurrences of marine invertebrates, including brachiopods and bivalves (Figs. 2–3). This long recognized assemblage is related to the *Eurydesma* fauna (Oliveira, 1927; Rocha-Campos and Rosler, 1978; Neves et al., 2014a, 2014b; Taboada et al., 2016), which implies that the Passinho Shale represents the record of the "*Eurydesma* transgression", as proposed by Dickins (1985), into the Paraná Basin. The paleotransport to SW recorded in the studied succession, in addition to the lateral changes of facies observed in the stratigraphic framework, indicates that this transgression came from the south.

Poorly diversified *Eurydesma* assemblages are also recognized in southwest Africa, interbedded with glaciomarine deposits of the Dwyka Group, in the Aranos Basin of Namibia (Dickins, 1961; Taboada et al., 2016). A cross-basin correlation permitted by the presence of the *Eurydesma* fauna thus shows that the Passinho Shale correlates with a relatively thick shale interval present in the Karoo and Kalahari basins, referred to as the Hardap Shale Member in the Kalahari Basin (Fig. 10; Dickins, 1961; SACS (South African Committee for Stratigraphy), 1980; Visser, 1997; Bangert et al., 1999; Stollhofen et al., 2000, 2008). This unit defines the top of the "Deglaciation Sequence 3" of

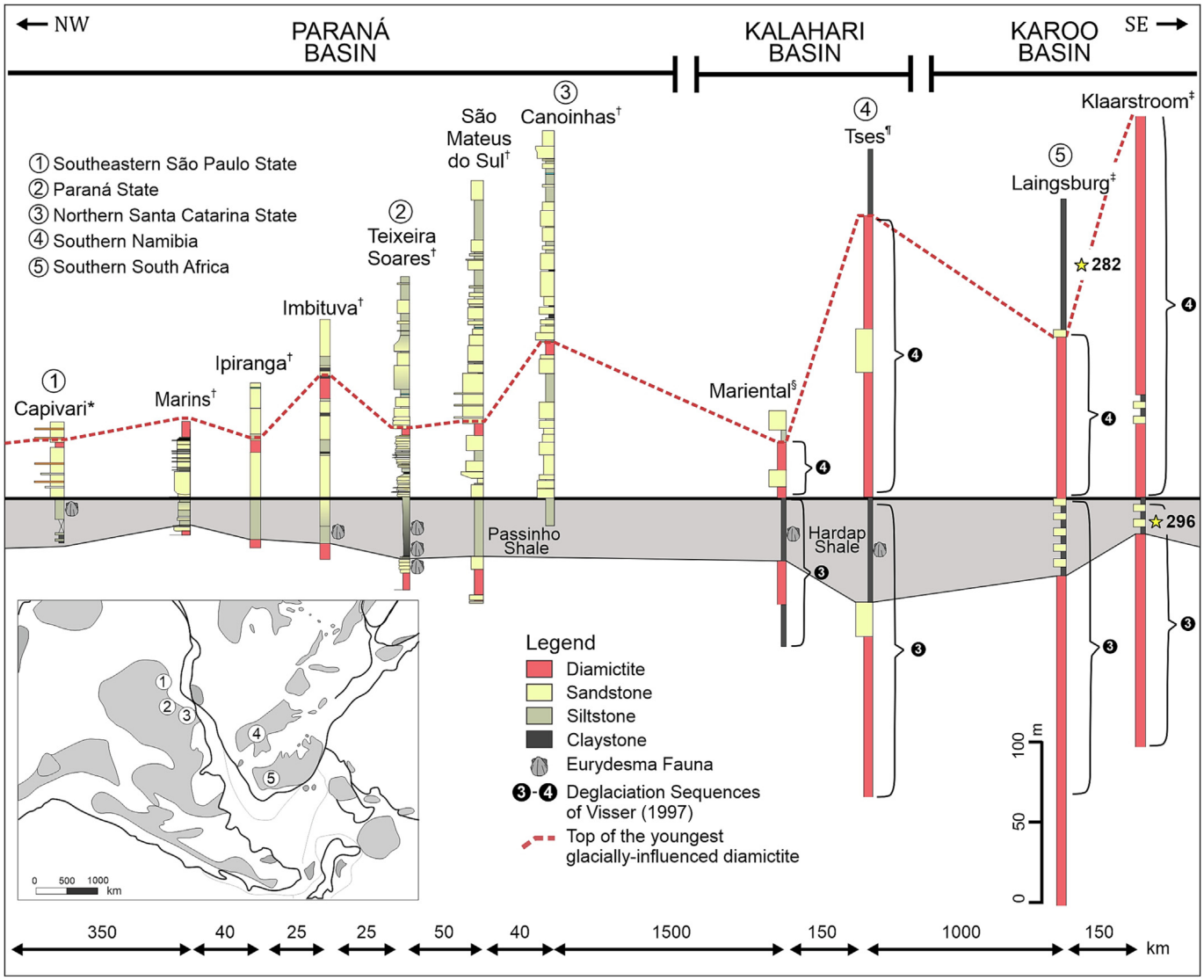

Fig. 10. Cross-basinal correlation panel of the "Eurydesma transgression" in SW Gondwana. The top of the shaly interval is used as datum. Symbols: *Modified from (Mendes, 1952); †well cores: RS-02-01/80 (Marins), PP-17-PR (Ipiranga), IV-10-PR (Imbituva), PP-16-PR (Teixeira Soares), PP-13-PR (São Mateus do Sul) and PP-11-SC (Canoinhas); §modified from Stollhofen et al. (2000); ¶modified from Visser (1997); ‡modified from Griffis et al. (2019a, 2019b). Sections are not to horizontal scale. Yellow stars are CA-TIMS ages (Ma) from Griffis et al. (2019a, 2019b).

the Dwyka Group (Visser, 1997). According to Stollhofen et al. (2000), the Hardap Shale thins westward, which is consistent with the thicknesses of the Passinho Shale observed in the Paraná Basin, that is about 40 m thinner compared to the equivalent unit in southwest Africa.

The age of the *Eurydesma* transgression is well constrained in the African side, assigned to the early Permian (Stollhofen et al., 2000; Stollhofen et al., 2008). Recent high-precision U–Pb CA-TIMS dating of volcaniclastic deposits, however, temporally refined this event in the Karoo Basin, indicating a middle Asselian age for the correspondent shale unit found in the Klaarstroom locality (296.41 Ma; Griffis et al., 2019a). In the absence of geochronological control for the stratigraphic interval bearing the *Eurydesma* assemblages in the study area and considering its proximity to basins in southwest Africa that show the equivalent fossiliferous (shale) interval and high-precision ages, we are extending the early Asselian age (Griffis et al., 2019a) to the Paraná Basin.

Furthermore, the correlation based on the presence of the *Eurydesma* fauna allows us to infer that the lower diamictite of U1 can be correlated with the "Deglaciation Sequence 3" (Visser, 1997) of the southern African basins, which is capped by the "Deglaciation Sequence 4" interval that must correspond to the U3 of the study area (Fig. 10).

5.4. Synthesis

It follows from the above that the terminal deglaciation in the study area occurred during the beginning of the Permian, different from the southernmost part of the basin, whose final deglaciation occurred prior to the Carboniferous–Permian boundary (Cagliari et al., 2016; Griffis et al., 2018, 2019a).

In the absence of radiometric ages in the study area, an early Permian age for the studied interval is supported by the floristic and faunal record of interglacial deposits of U2 by means of intrabasinal and cross-basinal correlations. More importantly, this points to a diachronous ending of the LPIA, besides suggesting that the glacial–postglacial transition is progressively older southward.

Moreover, our results support the idea that glaciation and deglaciation in western Gondwana were not associated with a continental-scale ice sheet. Rather, the coexistence of glaciated and non-glaciated areas within the same basin points to smaller and diachronous ice lobes. The results of the present paper also suggest the alternation of glacial and non-glacial conditions arranged in cycles of higher frequency than previously envisioned, and that the interglacial episode was warm enough to support coastal plains covered by plant communities.

Regarding the paleobotanical record of the analyzed interval, the floral change that occurred after the "*Eurydesma* transgression" should be highlighted. Initially, the P–G Flora that appears around the Carboniferous–Permian boundary and marks the beginning of the record of the "*Glossopteris* Flora" in the basin, is replaced by the G–B Flora that corresponds to plant assemblages typically associated with economically exploited coal seams that are common throughout the Rio Bonito Formation.

The main floristic changes from the P–G Flora to the G–B Flora include: (i) the disappearance of *Botrychiopsis*, a relictual plant from the Carboniferous, when it was a common and widely distributed element throughout Gondwana (Pinheiro et al., 2015), and (ii) the appearance of true ferns, with *Pecopteris* and *Sphenopteris*-type foliages, and sphenophyllalean sphenopsids (*Sphenophyllum*-type foliage). *Botrychiopsis* was a plant known to be well adapted to the main glacial interval of the LPIA that occurred in between the late Mississippian and late Pennsylvanian, from which it is believed to be the main element of the "Tundra" type vegetation during the Pennsylvanian of Australia (Retallack, 1980). In turn, pecopterid ferns and sphenophyllaleans are considered invaders originated in the Carboniferous tropics that emigrated from lower latitudes, advancing as the glacial influence retreated in the different regions of Gondwana (Archangelsky and Arrondo, 1971; Iannuzzi, 2010).

In this way, the above-mentioned plants in particular have an inverse paleoclimatic meaning, insofar as the presence of *Botrychiopsis* represents the existence of sufficiently cold-to-mild climatic conditions that still allowed its survival. The emergence and expansion of pecopterids and sphenophyllaleans would indicate warmer conditions that made it possible for them to invade and flourish in the midst of lowland vegetation already dominated by glossopterids throughout Permian.

In any case, if the changes in taxonomic composition that occurred from the P–G Flora to the G–B Flora can be attributed to a progressive warming (=climate change), they were also undoubtedly brought about by the remarkable rise in sea level (="*Eurydesma* transgression"). It is known that significant sea elevations which inundate coastal plains (lowlands) and destroy most of their terrestrial environments are events that can provide the replacement of taxa (species) in plant communities (DiMichele et al., 1996).

Fig. 11 summarizes the above results and interpretations as an attempt to establish a scheme to be used in future studies on sedimentary sequences in this part of the basin and/or for proposals for correlations with other areas of the Paraná and surrounding basins, i.e., in South America and southern Africa. Nevertheless, new geochronological data in the eastern margin of the Paraná Basin are needed to refine this scheme, as well as to permit direct correlations with adjacent dated successions.

6. Conclusions

- The glacial–postglacial transition in the eastern margin of the Paraná Basin comprises two deglaciation sequences (U1 and U3) interspersed with interglacial deposits (U2) assigned to the Itararé Group. The younger deglaciation is abruptly capped by postglacial deposits of the Rio Bonito Formation (U4).
- The correlation of the *Eurydesma* fauna-containing Passinho Shale with equivalent successions with age control in southern Africa, allowed the positioning of both deglaciations of the Taciba Formation in the earliest Permian, i.e., Asselian.
- There are two interglacial floras recognized in the study area; the first is dominated by *Botrychiopsis*, *Phyllotheca* and *Gangamopteris* elements and associated with the P–G Flora, correlating southwards with the postglacial floras of Quitéria and Candiota, whose absolute ages constrain their occurrence to the earliest Asselian; the second one overlaps the "*Eurydesma* transgression" and has elements such as *Pecopteris* and *Sphenophyllum*, thus corresponding to the G–B Flora and considered the oldest record of this type of flora that extends upwards throughout the Rio Bonito Formation.
- A younger deglaciation event, i.e., U3, is recorded only in the northeastern part of the basin, suggesting the existence of a glaciated source-area farther north of the Paraná and São Paulo states.
- The ultimate glacial demise and the turnover to a permanent postglacial stage are diachronous in the eastern belt of the Paraná Basin, and progressively older southward.

Supplementary data to this article can be found online at https://doi.org/10.1016/j.sedgeo.2023.106420.

Data availability

Data were made available as 3 Supplementary data files.

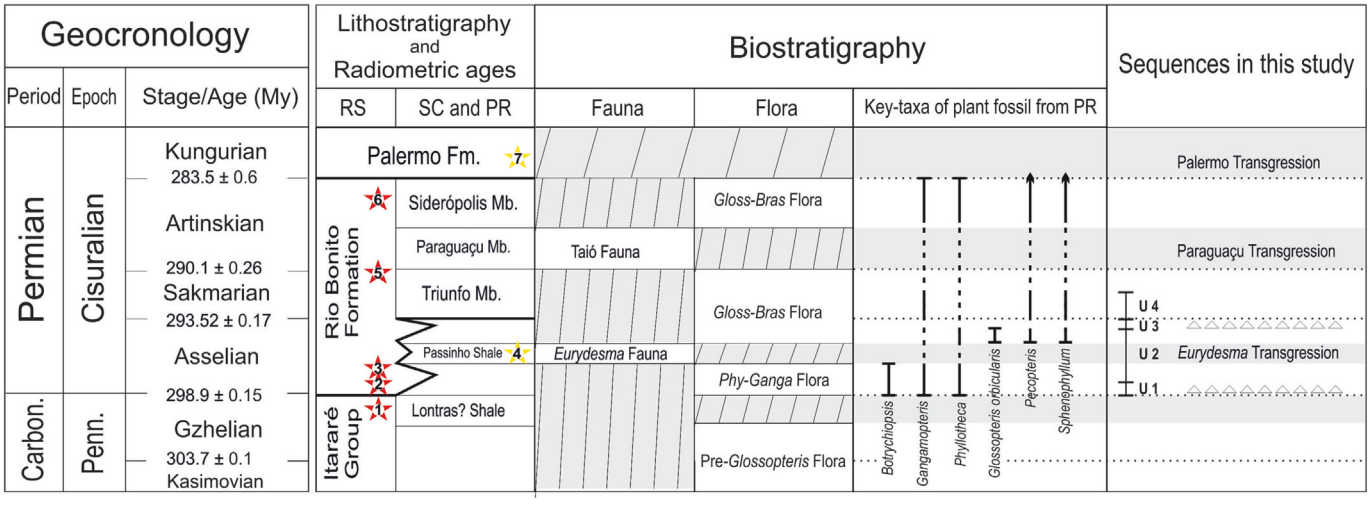

Fig. 11. Chronostratigraphic chart of the interval analyzed in this study, summarizing the results and interpretations obtained. Published high precision U–Pb radiometric ages: 1. Capané, uppermost Itararé Group, RS, Paraná Basin, 301.809 ± 0.224. 2. Candiota coalfield, Rio Bonito Formation, RS, Paraná Basin, 298.23 + 0.31 Ma, 297.77 + 0.35/−0.59 Ma, 297.58 + 0.68/−1.4 Ma (Griffis et al., 2018); 3. Quitéria Outcrop, Rio Bonito Formation, RS, Paraná Basin, 296.97 + 0.45/−0.72 Ma (Griffis et al., 2018); 4. Hardap Shale, in Klaarstroom, Karoo Basin, 296.41 + 0.27/−0.35 Ma (Griffis et al., 2019a); 5. Recreio Mine, Rio Bonito Formation, RS, Paraná Basin, 290.36 + 0.4/−0.32 Ma (Griffis et al., 2018); 6. Faxinal Mine, Rio Bonito Formation, RS, Paraná Basin, 285.42 + 1.2/−2.1 Ma (Griffis et al., 2018); 7. Lowermost Ecca Group, in Laingsburg, Karoo Basin, 282.17 + 0.32/−0.44 Ma (Griffis et al., 2019a). Floras according to Iannuzzi and Souza (2005): Phy-Ganga = *Phyllotheca–Gangamopteris*, Gloss-Bras = *Glossopteris–Brasilodendron*. Relative age of the Taió Fauna according to Holz et al. (2010). U1-U4 = Sequences determined in this study. Triangles lined up horizontally = diamictites. Carbon. = Carboniferous, Penn. = Pennsylvanian.

Declaration of competing interest

The authors declare that they have no known competing financial interests or personal relationships that could have appeared to influence the work reported in this paper.

Acknowledgements

This work is part of the Ph.D. project conducted by the first author and composes one chapter of the respective thesis. The research was financed in part by the Coordenação de Aperfeiçoamento de Pessoal de Nível Superior – Brasil (CAPES) – Finance Code 001, by the Brazilian National Council for Scientific and Technological Development (CNPq, grants 461650/2014-2 and 430096/2016-0), the U.S. National Science Foundation to I.P.M. (EAR1729882) and Petróleo Brasileiro S/A (Petrobras, grant 2016/00284-7). F.V. and R.I. are research fellows of the CNPq (PQ 302842/2017-9 and PQ 313946/2021-3, respectively). We thank Companhia de Pesquisa de Recursos Minerais (CPRM) for having allowed the access to well cores in Araraquara (São Paulo State) and the extinct MINEROPAR for having made available data from the "Projeto Carvão". The Society for Sedimentary Geology (SEPM) is further thanked for providing funding to T.E. Mottin. This paper was greatly improved by the feedback provided by two anonymous reviewers.

References

Almeida, F.F.M. de, 1945. Episódio da última época inter-glacial Permo Carbonífera no Paraná. Divisão Geologia e Mineralogia - Notas Preliminares e Estudos 27, 1–20.

Archangelsky, S., Arrondo, O.G., 1971. Paleophytologia Kurtziana III. 2. Estudio sobre el género Botrychiopsis Kurtz (=Gondwanidium Gothan) del Carbónico y Pérmico gondwánico. Ameghiniana 8, 189–227.

Bangert, B., Stollhofen, H., Lorenz, V., Armstrong, R., 1999. The geochronology and significance of ash-fall tuffs in the glaciogenic Carboniferous–Permian Dwyka Group of Namibia and South Africa. Journal of African Earth Sciences 29, 33–49. https://doi.org/10.1016/S0899-5362(99)00078-0.

Bernardes-de-Oliveira, M.E.C., Kavali, P.S., Mune, S.E., Shivanna, M., Souza, P.A., Iannuzzi, R., Jasper, A., Hoelzel, A., Boardman, D.R., Rohn, R., Ricardi-Branco, F., 2016. Pennsylvanian–Early Cisuralian interglacial macrofloristic succession in Paraná Basin of the State of São Paulo. Journal of South American Earth Sciences 72, 351–374. https://doi.org/10.1016/j.jsames.2016.09.004.

Boulton, G.S., 1990. Sedimentary and sea level changes during glacial cycles and their control on glacimarine facies architecture. Geological Society Special Publication 53, 15–52.

Boyd, R., Dalrymple, B.A., Zaitlin, B.A., 2006. Estuary and incised valley facies models. In: Posamentier, H.W., Walker, R.G. (Eds.), Facies Models Revisited. SEPM Special Publication, pp. 171–234.

Brandt, D., Ernesto, M., Constable, C., Franco, D.R., Weinschutz, L.C., Rodrigues, P.O.C., Hinnov, L., Jaqueto, P., Strauss, B.E., Feinberg, J., Franco, P.V.P., Zhao, X., 2019. New Late Pennsylvanian paleomagnetic results from Paraná Basin (Southern Brazil): is the recent giant Gaussian process model valid kiaman superchron? Journal of Geophysical Research - Solid Earth 124, 6223–6242.

Buatois, L.A., Mángano, M.G., Carr, T.R., 1999. Sedimentology and ichnology of paleozoic estuarine and shoreface reservoirs, morrow sandstone, lower Pennsylvanian of southwest Kansas, USA. Current Research in Earth Sciences 243, 1–35. https://doi.org/10.17161/cres.v0i243.11783.

Cagliari, J., Lavina, E.L.C., Philipp, R.P., Tognoli, F.M.W., Basei, M.A.S., Faccini, U.F., 2014. New Sakmarian ages for the Rio Bonito formation (Paraná Basin, southern Brazil) based on LA-ICP-MS U–Pb radiometric dating of zircons crystals. Journal of South American Earth Sciences 56, 265–277. https://doi.org/10.1016/j.jsames.2014.09.013.

Cagliari, J., Philipp, R.P., Buso, V.V., Netto, R.G., Klaus Hillebrand, P., da Cunha Lopes, R., Stipp Basei, M.A., Faccini, U.F., 2016. Age constraints of the glaciation in the Paraná Basin: evidence from new U–Pb dates. Journal of the Geological Society, London 173, 871–874. https://doi.org/10.1144/jgs2015-161.

Cagliari, J., Schmitz, M.D., Tedesco, J., Trentin, F.A., Lavina, E.L.C., 2023. High precision U-Pb geochronology and Bayesian age-depth modeling of the glacial-postglacial transition of the southern Paraná Basin: detailing the terminal phase of the Late Paleozoic Ice Age on Gondwana. Sediment. Geol. 451, 106397.

Carvalho, A.H., Vesely, F.F., 2017. Facies relationshipsrecorded in a Late Paleozoic fluvio-deltaic system (Paraná Basin, Brazil): insights into the timing and triggers of subaqueous sediment gravity flows. Sedimentary Geology 352, 45–62.

Castro, J.C., 1991. A evolução dos sistemas glacial, marinho e deltaico das formações Rio do Sul e Rio Bonito/Membro Triunfo (Eopermiano), sudeste da Bacia do Paraná. Universidade Estadual Paulista-IGCE (146pp.).

Cúneo, N.R., 1996. Permian phytogeography in Gondwana. Palaeogeography, Palaeoclimatology, Palaeoecology 125, 75–104. https://doi.org/10.1016/S0031-0182(96)00025-9.

Dashtgard, S.E., Gingras, M.K., MacEachern, J.A., 2009. Tidally modulated shorefaces. Journal of Sedimentary Research 79, 793–807.

Derby, O.A., 1878. A geologia da região diamantífera da Província do Paraná. Arquivos do Museu Nacional 3, 89–96.

Dickins, J.M., 1961. Eurydesma and Peruvispira from the Dwyka beds of SA. Palaeontology 4, 138–148.

Dickins, J.M., 1985. Late Paleozoic glaciation. BMR Journal of Australian Geology and Geophysics 9, 163–169.

Dietrich, P., Ghienne, J.F., Schuster, M., Lajeunesse, P., Nutz, A., Deschamps, R., Roquin, C., Duringer, P., 2017. From outwash to coastal systems in the Portneuf–Forestville deltaic complex (Québec North Shore): anatomy of a forced regressive deglacial sequence. Sedimentology 64, 1044–1078. https://doi.org/10.1111/sed.12340.

DiMichele, W.A., Pfefferkorn, H.W., Phillips, T.L., 1996. Persistence of Late Carboniferous tropical vegetation during glacially driven climatic and sea-level fluctuations. Palaeogeograpgy, Palaeoclimatology, Palaeoecology 125, 105–128.

Dolianiti, E., 1948. A Paleobotânica no Brasil. Departamento Nacional de Produção Mineral. Boletim Divisão de Geologia e Mineralogia 123, 1–87.

Dolianiti, E., 1954. Glossopteris orbicularis Feistmantel em Teixeira Soares. In: Lange, F.W. (Ed.), Volume Comemorativo Do 1° Centenário Do Estado Do Paraná. Comissão de Comemoração do centenário do Paraná, Curitiba, pp. 149–150.

Eyles, C.H., Eyles, N., França, A.B., 1993. Glaciation and tectonics in an active intracratonic basin: the Late Palaeozoic Itarare Group, Parana Basin, Brazil. Sedimentology 40, 1–25.

Fallgatter, C., Paim, P.S.G., 2019. On the origin of the Itararé Group basal nonconformity and its implications for the Late Paleozoic glaciation in the Paraná Basin, Brazil. Palaeogeography, Palaeoclimatology, Palaeoecology 531, 108225. https://doi.org/10.1016/j.palaeo.2017.02.039.

Fedo, C.M., Nesbitt, H.W., Young, G.M., 1995. Unraveling the effects of potassium metasomatism in sedimentary rocks and paleosols, with implications for paleoweathering conditions and provenance. Geology 23, 921–924. https://doi.org/10.1130/0091-7613(1995)023<0921.

Fernández, J.A., 2021. Revision of Botrychiopsis plantiana: a key species of the Gzhelian–Cisuralian in westernmost Gondwana. Ameghiniana 58, 1–11. https://doi.org/10.5710/AMGH.28.09.2020.3355.

Fernández, J.A., Césari, S.N., 2019. Leafy branches of Gangamopteris from the Gzhelian–Asselian of westernmost Gondwana. Comptes Rendus Palevol 18, 913–924. https://doi.org/10.1016/j.crpv.2019.10.004.

Fielding, C.R., Frank, T.D., Birgenheier, L.P., Rygel, M.C., Jones, A.T., 2008. Stratigraphic imprint of the Late Paleozoic Ice Age in eastern Australia: a record of alternating glacial and non-glacial climate regime. Journal of the Geological Society 165, 129–140.

Fielding, C.R., Frank, T.D., Birgenheier, L.P., 2022. A revised, late Paleozoic glacial time-space framework for eastern Australia, and comparisons with other regions and events. Earth-Science Reviews 236, 104263. https://doi.org/10.1130/abs/2022am-378410.

França, A.B., Potter, P.E., 1988. Estratigrafia, ambiente deposicional e análise de reservatório do Grupo Itararé (Permocarbonífero), Bacia do Paraná (Parte 1). Boletim de Geociências da Petrobrás 2, 147–191. https://doi.org/10.18356/0e75c030-ru.

Franco, D.R., Ernesto, M., Ponte-Neto, C.F., Hinnov, L.A., Berquó, T.S., Fabris, J.D., Rosière, C.A., 2012. Magnetostratigraphy and mid-palaeolatitude VGP dispersion during the Permo-Carboniferous Superchron: results from Paraná Basin (Southern Brazil) rhythmites. Geophysical Journal International 191, 993–1014.

Gama Jr., E.G., Perinotto, J.A.J., Ribeiro, H.J.P.S., Padula, E.K., 1992. Contribuição ao estudo da ressedimentação no Subgrupo Itararé: tratos de fácies e hidrodinâmica deposicional. Revista Brasileira de Geociencias 22 (2), 228–236.

Gastaldo, R.A., DiMichele, W.A., Pfefferkorn, H.W., 1996. Out of the icehouse into the greenhouse: a late Paleozoic analog for modern global vegetational change. GSA Today 6, 1–7.

Goddéris, Y., Donnadieu, Y., Carretier, S., Aretz, M., Dera, G., MacOuin, M., 2017. Onset and ending of the late Palaeozoic ice age triggered by tectonically paced rock weathering. Nature Geoscience 10, 382–386.

Griffis, N.P., Mundil, R., Montañez, I.P., Isbell, J., Fedorchuk, N., Vesely, F., Iannuzzi, R., Yin, Q.Z., 2018. A new stratigraphic framework built on U–Pb singlezircon TIMS ages and implications for the timing of the penultimate icehouse (Paraná Basin, Brazil). Bulletin Geological Society of America 130, 848–858. https://doi.org/10.1130/B31775.1.

Griffis, N.P., Montañez, I.P., Mundil, R., Richey, J., Isbell, J., Fedorchuk, N., Linol, B., Iannuzzi, R., Vesely, F., Mottin, T., da Rosa, E., Keller, B., Yin, Q.-Z., 2019a. Coupled stratigraphic and U–Pb zircon age constraints on the late paleozoic icehouse-to-greenhouse turnover in south-central gondwana. Geology 47, 1146–1150. https://doi.org/10.1130/G46740.1.

Griffis, N.P., Montañez, I.P., Fedorchuk, N., Isbell, J., Mundil, R., Vesely, F., Weinshultz, L., Iannuzzi, R., Gulbranson, E., Taboada, A., Pagani, A., Sanborn, M.E., Huyskens, M., Wimpenny, J., Linol, B., Yin, Q.Z., 2019b. Isotopes to ice: constraining provenance of glacial deposits and ice centers in west-central Gondwana. Palaeogeography, Palaeoclimatology, Palaeoecology 531, 108745. https://doi.org/10.1016/j.palaeo.2018.04.020.

Griffis, N., Montañez, I., Mundil, R., Le Heron, D., Dietrich, P., Kettler, C., Linol, B., Mottin, T., Vesely, F., Iannuzzi, R., Huyskens, M., Yin, Q.-Z., 2021. High-latitude ice and climate control on sediment supply across SW Gondwana during the late Carboniferous and early Permian. GSA Bulletin 1–12. https://doi.org/10.1130/b35852.1.

Guerra-Sommer, M., Rodrigues, C.G., David, C.A.R., Oliveira, L.M. de, 1981. Análise do conteúdo paleobotânico de pelitos fossilíferos (Formação Rio Bonito) da área de Ribeirão Novo, Paraná. 3o Simpósio Regional de Geologia, pp. 180–189.

Gugliotta, M., Flint, S.S., Hodgson, D.M., Veiga, G.D., 2015. Stratigraphic record of river-dominated crevasse subdeltas with tidal influence (Lajas Formation, Argentina). Journal of Sedimentary Research 85, 265–284. https://doi.org/10.2110/jsr.2015.19.

Holz, M., França, A.B., Souza, P.A., Iannuzzi, R., Rohn, R., 2010. A stratigraphic chart of the Late Carboniferous/Permian succession of the eastern border of the Paraná Basin,

Brazil, South America. Journal of South American Earth Sciences 29, 381–399. https://doi.org/10.1016/j.jsames.2009.04.004.
Iannuzzi, R., 2010. The flora of Early Permian coal measures from the Paraná Basin in Brazil: a review. International Journal of Coal Geology 83, 229–247. https://doi.org/10.1016/j.coal.2010.05.009.
Iannuzzi, R., 2013. The Carboniferous–Permian floral transition in the Paraná Basin. Bulletin New Mexico Museum of Natural History and Science 60, 132–136.
Iannuzzi, R., 2021. Fitoestratigrafia dos estados do Rio Grande do Sul e de Santa Catarina. (Org.)In: Jelinek, A.R., Sommer, C.A. (Eds.), Contribuições à Geologia do Rio Grande doSul e de Santa Catarina, 1ed. Compasso Lugar-Cultura, Porto Alegre, pp. 241–255.
Iannuzzi, R., Souza, P.A., 2005. Floral succession in the Lower Permian deposits of the Brazilian Paraná Basin: an up-to-date overview. In: Lucas, S.G., Zigler, K.E. (Eds.), The Nonmarine Permian: New Mexico Museum of Natural History and Science Bulletin vol. 30, pp. 144–149.
Iannuzzi, R., Souza, P.A., Holz, M., 2007a. Lower Permian post-glacial succession in the southernmost Brazilian Paraná Basin: stratigraphy and floral (macro and micro) record. 4th European Meeting on the Palaeontology and Stratigraphy of Latin America, pp. 207–212.
Iannuzzi, R., Souza, P.A., Scherer, C.M.S., Holz, M., 2007b. Plantas fósseis na Bioestratigrafia dos Depósitos Permianos do Rio Grande do Sul. (Org.)In: Iannuzzi, R., Frantz, J.C. (Eds.), 50 Anos de Geologia. Instituto de Geociências. Contribuições. Comunicação e Identidade, Porto Alegre, pp. 265–281.
Iannuzzi, R., Souza, P.A., Holz, M., 2010. Stratigraphic and paleofloristic record of the Lower Permian post-glacial succession in the southern Brazilian. Geological Society of America Special Paper 468, 113–132.
Isbell, J.L., Miller, M.F., Wolfe, K.L., Lenaker, P.A., 2003. Timing of late Paleozoic glaciation in Gondwana: was glaciation responsible for the development of northern hemisphere cyclothems? Geological Society of America Special Papers 370, 5–24. https://doi.org/10.1130/0-8137-2370-1.5.
Isbell, J.L., Koch, Z.J., Szablewski, G.M., Lenaker, P.A., 2008. Permian glacigenic deposits in the Transantarctic Mountains, Antarctica. Geological Society of America Special Papers 441, 59–70. https://doi.org/10.1130/2008.2441(04).
Isbell, J.L., Henry, L.C., Gulbranson, E.L., Limarino, C.O., Fraiser, M.L., Koch, Z.J., Ciccioli, P.L., Dineen, A.A., 2012. Glacial paradoxes during the late Paleozoic ice age: evaluating the equilibrium line altitude as a control on glaciation. Gondwana Research 22, 1–19. https://doi.org/10.1016/j.gr.2011.11.005.
Isbell, J.L., Vesely, F.F., Rosa, E.L.M., Pauls, K.N., Fedorchuk, N.D., Ives, L.R.W., McNall, N.B., Litwin, S.A., Borucki, M.K., Malone, J.E., Kusick, A.R., 2021. Evaluation of physical and chemical proxies used to interpret past glaciations with a focus on the late Paleozoic Ice Age. Earth-Science Reviews 221, 103756.
Jasper, A., Guerra-Sommer, M., Cazzulo-Klepzig, M., Menegat, R., 2003. The Botrychiopsis genus and its biostratigraphic implications in Southern Paraná Basin. Anais da Academia Brasileira de Ciências 75, 513–535. https://doi.org/10.1590/S0001-37652003000400009.
Knaust, D., 2017. Atlas of Trace Fossils in Well Core - Appearance Taxonomy and Interpretation. first ed. Springer Cham (209 pp.).
Kneller, B., Milana, J.P., Buckee, C., al Ja'aidi, O., 2004. A depositional record of deglaciation in a paleofjord (Late Carboniferous [Pennsylvanian] of San Juan Province, Argentina): the role of catastrophic sedimentation. Bulletin of the Geological Society of America 116, 348–367. https://doi.org/10.1130/B25242.1.
Lambeck, K., 1991. Glacial rebound and sea-level change in the British Isles. Terra Research 3, 379–389.
Lange, F.W., 1954. Estratigrafia e idade geológica da Série Tubarão. Arquivos do Museu Paranaense (Série Geologia). vol. 2.
Limarino, C.O., Césari, S.N., Spalletti, L.A., Taboada, A.C., Isbell, J.L., Geuna, S., Gulbranson, E.L., 2014. A paleoclimatic review of southern South America during the late Paleozoic: a record from icehouse to extreme greenhouse conditions. Gondwana Research 25, 1396–1421. https://doi.org/10.1016/j.gr.2012.12.022.
López-Gamundí, O., Limarino, C.O., Isbell, J.I., Pauls, K., Césari, S.N., Alonso-Muruaga, P.J., 2021. The late Paleozoic Ice Age along the southwestern margin of Gondwana: facies models, age constraints, correlation and sequence stratigraphic framework. Journal of South American Earth Sciences 107, 103056.
Lowe, D.R., 1982. Sediment gravity flows II: depositional models with special reference tothe deposits of high density turbidity currents. Journal of Sedimentary Petrology 52 (1), 279–297.
Martini, I.P., Brookfield, M.E., 1995. Sequence analysis of Upper Pleistocene (Wisconsinan) glaciolacustrine deposits of the north-shore bluffs of Lake Ontario, Canada. Journal of Sedimentary Research 65B, 388–400. https://doi.org/10.1306/d426825c-2b26-11d7-8648000102c1865d.
Medeiros, R.A., Thomaz Filho, A., 1973. Fácies e ambientes deposicionais da Formação Rio Bonito. Anais Do 27° Congresso Brasileiro de Geologia. Aracajú, pp. 3–12.
Mendes, J.C., 1952. Faunula Permo-Carbonifera marinha de Capivari (Estado de São Paulo). Boletim da Faculdade de Filosofia Ciências e Letras Universidade de São Paulo. Geologia 7, 1–13.
Milani, E.J., 1997. Evolução tectono-estratigráfica da Bacia do Paraná e seu relacionamento com a geodinâmica Fanerozóica do Gondwana Sul-Ocidental. Curso Pós-Graduação em Geociências 255 2 vol.
Montañez, I.P., 2022. Current synthesis of the penultimate icehouse and its imprint on the Upper Devonian through Permian stratigraphic record. Geological Society of London, Special Publication 512, 213–245. https://doi.org/10.1144/sp512-2021-124.
Montañez, I.P., Poulsen, C.J., 2013. The late Paleozoic ice age: an evolving paradigm. Annual Review of Earth and Planetary Sciences 41, 629–656. https://doi.org/10.1146/annurev.earth.031208.100118.
Montañez, I.P., Tabor, J.J., Niemeier, D., DiMichele, W.A., Frank, T.D., Fielding, C.R., Isbell, J.J., Birgenheieer, I.P., Rygel, M.C., 2007. CO2-forced climate and vegetation instability during late Paleozoic deglaciation. Science 325, 87–91.
Mottin, T.E., 2022. Stratigraphic Record of Environmental Changes During the Late Paleozoic Glacial–Postglacial Transition in Northeastern Paraná Basin, Brazil. Universidade Federal do Paraná, Curitiba (Ph.D. thesis, 172 pp.).
Mottin, T.E., Vesely, F.F., 2021. Formação Taciba: última manifestação glacial no Paraná. Boletim Paranaense de Geociências 78, 65–82.
Mottin, T.E., Vesely, F.F., de Lima Rodrigues, M.C.N., Kipper, F., de Souza, P.A., 2018. The paths and timing of late Paleozoic ice revisited: new stratigraphic and paleo-ice flow interpretations from a glacial succession in the upper Itararé Group (Paraná Basin, Brazil). Palaeogeography, Palaeoclimatology, Palaeoecology 490, 488–504. https://doi.org/10.1016/j.palaeo.2017.11.031.
Mottin, T.E., Kipper, F., Vesely, F.F., de Souza, P.A., 2020. Palinoestratigrafia e paleoecologia da Formação Taciba (Grupo Itararé) na região de Ibaiti-PR, nordeste da Bacia do Paraná. Boletim Paranaense de Geosciencias 77, 32–39.
Mottin, T.E., Iannuzzi, R., Vesely, F.F., Montañez, I.P., Griffis, N., Canata, R.E., Barão, L.M., da Silveira, D.M., Garcia, A.M., 2022. A glimpse of a Gondwanan postglacial fossil forest. Palaeogeography, Palaeoclimatology, Palaeoecology 588. https://doi.org/10.1016/j.palaeo.2021.110814.
Mutti, E., Tinterri, R., Magalhaes, P.M., Basta, G., 2007. Deep-water turbidites and their equally important shallower water cousins. Search and Discovery article. Adapted From Extended Abstract Prepared for Presentation at AAPG Annual Convention, Long Beach, pp. 1–7.
Nesbitt, H.W., Young, G.M., 1982. Early proterozoic climates and plate motions inferred from major element chemistry of lutites. Nature 299, 715–717. https://doi.org/10.1038/299715a0.
Neves, J.P., Anelli, L.E., Pagani, M.A., Simões, M.G., 2014a. Late Palaeozoic South American pectinids revised: biostratigraphical and palaeogeographical implications. Alcheringa: An Australasian Journal of Palaeontology 38, 281–295. https://doi.org/10.1080/03115518.2014.870383.
Neves, J.P., Anelli, L.E., Simões, M.G., 2014b. Early Permian post-glacial bivalve faunas of the Itararé Group, Paraná Basin, Brazil: paleoecology and biocorrelations with South American intraplate basins. Journal of South American Earth Sciences 52, 203–233. https://doi.org/10.1016/j.jsames.2014.03.001.
Nio, S.D., Yang, C.S., 1991. Sea-level fluctuations and geometric variability of tide-dominatedsandbodies. Sedimentary Geology 70, 161–193.
Nutz, A., Ghienne, J.-F., Schuster, M., Dietrich, P., Roquin, C., Hay, M.B., Bouchette, F., Cousineau, P.A., 2015. Forced regressive deposits of a deglaciation sequence: example from the Late Quaternary succession in the Lake Saint-Jean basin (Québec, Canada). Sedimentology 62, 1573–1610. https://doi.org/10.1111/sed.12196.
Oliveira, E., 1927. Geologia e Recursos Minerais do Estado do Paraná. Serviço Geológico e Mineralógico do Brasil.
Pinheiro, E.R.S., Gallego, J., Iannuzzi, R., Cúneo, R., 2015. First report of feeding traces in Permian Botrychiopsis leaves from Western Gondwana. Palaios 30, 613–619.
Posamentier, H.W., Martinsen, O.J., 2011. The character and genesis of submarine mass-transport deposits: insights from outcrop and 3D seismic data. In: Shipp, R.C., Weimer, P., Posamentier, H.W. (Eds.), Mass-transport Deposits in Deepwater Settings. SEPM Society for Sedimentary, pp. 7–38.
Powell, R., Domack, E., 2002. Modern glaciomarine environments. In: Menzies, J. (Ed.), Modern and Past Glacial Environments. Butterworth-Heinemann Ltd., Oxford, pp. 361–389.
Powell, C.McA, Li, Z.X., 1994. Reconstruction of the Panthalassan margin of Gondwanaland. In: Veevers, J.J., Powell, C.McA. (Eds.), Permian–Triassic Pangean Basins and Foldbelts along the Panthalassan Margin of Gondwanaland. Geological Society America, Memoir vol. 184, pp. 5–9.
Puigdomenech, C.G., Carvalho, B., Paim, P.S.G., Faccini, U.F., 2015. Lowstand turbidites and delta systems of the Itararé Group in the Vidal Ramos region (SC), southern Brazil. Brazilian Journal of Geology 44, 529–544. https://doi.org/10.5327/z2317488920140004002.
Read, C.B., 1941. Plantas fósseis do Neo-Paleozoico do Paraná e Santa Catarina. Monografia da Divisão Geologia e Mineralogia 12 (118 pp.).
Retallack, G.J., 1980. Late Carboniferous to Middle Triassic megafossil floras fromthe Sidney basin. In: Herbert, C., Helby, R. (Eds.), A Guide to the Sydney Basin. Geological Survey of the New South Wales Bulletin vol. 26, pp. 384–430.
Ricardi-Branco, F.S., 1997. Tafoflora Gondvânica do Membro Triunfo FOrmação Rio Bonito (Eopermiano), no Município de Figueira, PR. Universidade de São Paulo.
Ricardi-Branco, F., 2004. The paleoflora of Figueira in the context of the neopaleozoic of the Paraná Basin, Brazil. Terrae 1, 44–51.
Richey, J.D., Montañez, I.P., Goddéris, Y., Looy, C.V., Griffis, N.P., DiMichele, W.A., 2020. Influence of temporally varying weatherability on CO2-climate coupling and ecosystem change in the late Paleozoic. Climate of the Past 16, 1759–1775.
Rigby, J.F., 1972. The Upper Palaeozoic Flora at Lauro Müller Santa Catarina, southern Brazil. Anais da Academia Brasileira de Ciências 44 (Supl), 279–293.
Rocha-Campos, A.C., 1967. The Tubarão Group in the Brazilian Portion of Paraná Basin. In: Bigarella, J.J., Becker, R.D., Pinto, I.D. (Eds.), Problems in Brazilian Gondwana Geology, I. International Symposium on the Gondwana Stratigraphy and Paleontology, Curitiba, pp. 27–102.
Rocha-Campos, A.C., Rosler, O., 1978. Late Paleozoic faunal and floral successions in the Paraná basin, southeastern Brazil. Boletim IG, Instituto de Geociencias 9, 1–16.
Rocha-Campos, A.C., dos Santos, P.R., Canuto, J.R., 2008. Late Paleozoic glacial deposits of Brazil: Paraná Basin. Special Paper Geological Society of America 441, 97–114. https://doi.org/10.1130/2008.2441(07).
Rodrigues, M.C.N.L., Trzaskos, B., Alsop, G.I., Vesely, F.F., 2020. Making a homogenite: an outcrop perspective into the evolution of deformation within mass-transport deposits. Marine and Petroleum Geology 112, 104033. https://doi.org/10.1016/j.marpetgeo.2019.104033.
Rodrigues, M.C.N.L., Trzaskos, B., Alsop, G.I., Farias, F., Mottin, T.E., Schemiko, D.C.B., 2021. Statistical analysis of structures commonly used to determine palaeoslopes from

within mass transport deposits. Journal of Structural Geology 151, 104421. https://doi.org/10.1016/j.jsg.2021.104421.
Rohn, R., Longhim, M.E., Bernardes-de-Oliveira, M.E., Navarro, G.R.B., 2000. Nova ocorrência fitofossilífera neocarbonífera-eopermiana do subgrupo itararé. Revista da Universidade Guarulhos, Geociências 57–61.
Rosa, L.E.M., Vesely, F.F., França, A.B., 2016. A review on late Paleozoic ice-relatederosional landforms of the Paraná Basin: origin and paleogeographical implications. Brazilian Journal of Geology 46 (2), 147–166.
Rosa, E.L.M., Vesely, F.F., Isbell, J.L., Kipper, F., Fedorchuk, N.D., Souza, P.A., 2019. Constraining the timing, kinematics and cyclicity of Mississippian–Early Pennsylvanian glaciations in the Paraná Basin, Brazil. Sedimentary Geology 384, 29–49. https://doi.org/10.1016/j.sedgeo.2019.03.001.
Rösler, O., 1978. The Brazilian eogondwanic floral succession. Boletim IG 9, 85. https://doi.org/10.11606/issn.2316-8978.v9i0p85-91.
Rossi, V.M., Steel, R.J., 2016. The role of tidal, wave and river currents in the evolution of mixed-energy deltas: example from the Lajas Formation (Argentina). Sedimentology 63, 824–864.
SACS (South African Committee for Stratigraphy), 1980. Stratigraphy of South Africa. Part 1: lithostratigraphy of the Republic of South Africa, South West Africa/Namibia and the Republics of Bophuthatswana, Transkei and Venda. Geological Survey South Africa Handbook. vol. 8, p. l-690 (L.E. Kent, Compiler).
Salvador, A., 2013. Lithostratigraphic units. In: Salvador, A. (Ed.), International Stratigraphic Guide: A Guide to Stratigraphic Classification, Terminology, and Procedure. Geological Society of America, pp. 31–44.
Santos, P.R., Rocha-Campos, A.C., Canuto, J.R., 1996. Patterns of late Palaeozoic deglaciation in the Paraná Basin, Brazil. Palaeogeography Palaeoclimatology Palaeoecology 125, 165–184.
Schemiko, D.C.B., Vesely, F.F., Rodrigues, M.C.N.L., 2019. Deepwater to fluvio-deltaic stratigraphic evolution of a deglaciated depocenter: the early Permian Rio do Sul and Rio Bonito formations, southern Brazil. Journal of South American Earth Sciences 95, 102260. https://doi.org/10.1016/j.jsames.2019.102260.
Schneider, R.L., Muhlmann, H., Tommazi, E., Medeiros, R.A., Daemon, R.F., Nogueira, A.A., 1974. Revisão Estratigráfica da Bacia do Paraná. Anais Do XXVIII Congresso, pp. 41–65.
Shanmugam, G., 2006. Deep-water Processes and Facies Models: Implications for Sandstone Petroleum Reservoirs. Elsevier, Amsterdam, p. 496.
Soares, P.C., Landim, P.M.B., Fúlfaro, V.J., 1977. Tectonic cycles and sedimentary sequences in the Brazilian intracratonic basins. Geological Society of America Bulletin Boulder 89 (2), 181–191.
Sobiesiak, M.S., Kneller, B., Alsop, G.I., Milana, J.P., 2018. Styles of basal interaction beneath mass transport deposits. Marine and Petroleum Geology 98, 629–639.
Souza, P.A., Boardman, D.R., Premaor, E., Félix, C.M., Bender, R.R., Oliveira, E.J., 2021. The Vittatina costabilis Zone revisited: new characterization and implications on the Pennsylvanian–Permian icehouse-to-greenhouse turnover in the Paraná Basin, Western Gondwana. Journal of South American Earth Sciences 106, 102968. https://doi.org/10.1016/j.jsames.2020.102968.
Stollhofen, H., Stanistreet, I.G., Bangert, B., Grill, H., 2000. Tuffs, tectonism and glacially related sea-level changes, Carboniferous–Permian, southern Namibia. Palaeogeography, Palaeoclimatology, Palaeoecology 161, 127–150. https://doi.org/10.1016/S0031-0182(00)00120-6.
Stollhofen, H., Werner, M., Stanistreet, I.G., Armstrong, R.A., 2008. Single-zircon U–Pb dating of Carboniferous–Permian tuffs, Namibia, and intercontinental deglaciation cycle framework. Special Paper Geological Society of America 441, 83–96.
Taboada, A.C., Neves, J.P., Weinschütz, L.C., Pagani, M.A., Simões, M.G., 2016. Eurydesma–Lyonia fauna (Early Permian) from the Itararé group, Paraná Basin (Brazil): a paleobiogeographic W–E trans-Gondwanan marine connection. Palaeogeography, Palaeoclimatology, Palaeoecology 449, 431–454. https://doi.org/10.1016/j.palaeo.2016.02.022.
Tänavsuu-Milkeviciene, K., Plink-Björklund, P., 2009. Recognizing tide-dominated versus tide-influenced deltas: middle Devonian strata of the Baltic Basin. Journal of Sedimentary Research 79, 887–905.
Tybusch, G.P., Iannuzzi, R., Rösler, O., 2012. Estudo das glossopteríideas do afloramento de Rio da Estiva, estado de Santa Catarina (Permiano Inferior da Bacia do Paraná). Pesquisas em Geociências 39, 23–33.
Valdez Buso, V., Aquino, C.D., Paim, P.S.G., de Souza, P.A., Mori, A.L., Fallgatter, C., Milana, J.P., Kneller, B., 2019. Late Palaeozoic glacial cycles and subcycles in western Gondwana: correlation of surface and subsurface data of the Paraná Basin, Brazil. Palaeogeography, Palaeoclimatology, Palaeoecology 531, 108435. https://doi.org/10.1016/j.palaeo.2017.09.004.
Vesely, F.F., Assine, M.L., 2004. Seqüências e Tratos de Sistemas Deposicionais do Grupo Itararé, Norte do Estado do Paraná. Revista Brasileira de Geociencias 34, 219–230. https://doi.org/10.25249/0375-7536.2004342219230.
Vesely, F.F., Assine, M.A., 2006. Deglaciation sequences in the Permo–Carboniferous Itararé Group, Paraná Basin, southern Brazil. Journal of South American Earth Sciences 22, 156–168. https://doi.org/10.1016/j.jsames.2006.09.006.
Vesely, F.F., Trzaskos, B., Kipper, F., Assine, M.L., Souza, P.A., 2015. Sedimentary record of a fluctuating ice margin from the Pennsylvanian of western Gondwana: Paraná Basin, southern Brazil. Sedimentary Geology 326, 45–63. https://doi.org/10.1016/j.sedgeo.2015.06.012.
Visser, J.N.J., 1989. The Permo-carboniferous Dwyka Formation of Southern Africa: deposition by a predominantly subpolar marine ice-sheet. Palaeogeography, Paleoclimatology, Palaeoecology 70, 377–391.
Visser, J.N.N., 1993. Sea-level changes in a back-arc-foreland transition: the late Carboniferous–Permian Karoo Basin of South Africa. Sedimentary Geology 83, 115–131.
Visser, J., 1994. The interpretation of massive rain-out and debris-flow diamictites from the glacial marine environment. In: Deynoux, M., Miller, J., Domack, E., Eyles, N., Fairchild, I., Young, G. (Eds.), Earth's Glacial Record. World and Regional Geology. Cambridge University Press, Cambridge, pp. 83–94 https://doi.org/10.1017/CBO9780511628900.007.
Visser, J.N.J., 1997. Deglaciation sequences in the Permo-Carboniferous Karoo and Kalahari basins of southern Africa: a tool in the analysis of cyclic glaciomarine basin fills. Sedimentology 44, 507–521. https://doi.org/10.1046/j.1365-3091.1997.d01-35.x.
Wang, P., Du, Y., Yu, W., Algeo, T.J., Zhou, Q., Xu, Y., Qi, L., Yuan, L., Pan, W., 2020. The chemical index of alteration (CIA) as a proxy for climate change during glacial–interglacial transitions in Earth history. Earth-Science Reviews 201, 103032. https://doi.org/10.1016/j.earscirev.2019.103032.
Wesolowski, L.J.N., Buatois, L.A., Mángano, M.G., Ponce, J.J., Carmona, N.B., 2018. Trace fossils, sedimentary facies and parasequence architecture from the Lower Cretaceous Mulichinco Formation of Argentina: the role of fair-weather waves in shoreface deposits. Sedimentary Geology 367, 146–163. https://doi.org/10.1016/j.sedgeo.2018.02.007.
Willis, B.J., Bhattacharya, S.L., Gabel, S.L., White, C.D., 1999. Architecture of a tideinfluencedriver delta in the Frontier Formation of central Wyoming, USA. Sedimentology 46, 667–688.
Zacharias, A.Á., 2004. Preenchimento de Vales Incisos por Associações de Fácies Estuarinas, Formação Rio Bonito, Nordeste do Paraná. Instituto de Geociências e Ciências Exatas (92 pp.).
Zacharias, A.A., Assine, M.L., 2005. Modelo de preenchimento de vales incisos por associações de fácies estuarinas, Formação Rio Bonito no norte do estado do Paraná. Revista Brasileira de Geociencias 35, 573–583. https://doi.org/10.25249/0375-7536.200535573583.